Decentralized State-Space Controller Design of a Large PHWR

by

Nafisah Khan

A Thesis Submitted in Partial Fulfillment
of the Requirements for the Degree of

Master of Applied Science

in

Nuclear Engineering

The Faculty of Energy Systems and Nuclear Science

University of Ontario Institute of Technology

November 2009

Abstract

The behaviour of a large nuclear reactor can be described with sufficient accuracy using a nodal model, like the spatial model of a 540 MWe large Pressurized Heavy Water Reactor (PHWR). This model divides the reactor into divisions or nodes to create a spatial model in order to control the xenon induced oscillations that occur in PHWRs. However, being such a large scale system, a 72^{nd}-order model, it makes controller design challenging. Therefore, a reduced order model is much more manageable. A convenient method of model reduction while maintaining the important dynamics characteristics of the process can be done by decoupling. Also, due to the nature of the system, decentralized controllers could serve as a better option because it allows each controller to be localized. This way, any control input to a zone only affects the desired zone and the zones most coupled with, thus not causing a respective change in neutron flux in the other zones.

In this thesis, three decentralized controllers were designed using the spatial model of a 540 MWe large PHWR. A decoupling algorithm was designed to divide the system into three partitions containing 20, 27, and 25 states each. Reduced order sub-systems were thus created to produce optimal decentralized controllers. An optimal centralized controller was created to compare both approaches. The decentralized versus centralized controllers' system responses were analyzed after a reactivity disturbance. A fail-safe study was done to highlight one of the advantages of decentralized controllers.

Keywords: Decentralized control, state-space control, spatial control, decoupling algorithm, reactor nodal core model, Large PHWR, liquid zone level control

Acknowledgements

First and foremost, I would like to thank God for all that He has given me. It is by His grace, love, and mercy, that I am able to achieve anything.

I would like to thank my supervisor, Dr. Lixuan Lu, for her continuous guidance and support.

I would like to thank my parents and siblings for their unconditional love, support, and encouragement throughout my studies.

Table of Contents

List of Tables

List of Figures

List of Appendices

Nomenclature

i and j subscripts to denote zones,

N number of zones in the reactor,

m_d number of delayed neutron precursor groups,

P power level, MW

$\rho_{exi,}$ reactivity related to the external control mechanism, mk

$\rho_{fi,}$ feedback due to fuel temperature, mk

ρ_{ci} feedback due to primary coolant temperature, mk

C delayed neutron precursors' concentration, n/cm^3

β total delayed neutron fractional yield,

λ_g decay constant for gth group of delayed neutron precursors, s^{-1}

X xenon concentration, n/cm^3

Σ_a thermal neutron absorption cross section, cm^{-1}

Σ_f thermal neutron fission cross section, cm^{-1}

l prompt neutron lifetime, s

E_{eff} energy liberated per fission, MJ

V' volume, cm

σ_x xenon microscopic thermal neutron absorption cross section, cm^2

α_{ij} coupling coefficient,

D diffusion coefficient, cm

υ thermal neutron speed, cm/s

Ψ_{ij} area of interface between ith and jth zones, cm^2

d_{ij} distance between ith and jth zones, cm

I iodine concentration, n/cm^3

γ_x xenon yield per fission

γ_I iodine yield per fission

λ_x xenon decay constant, s^{-1}

λ_I iodine decay constant, s^{-1}

T_f fuel temperature, K

T_c coolant temperature, K

T_1 coolant inlet temperature, K

P_g global power, MW

k_a, k_b, k_c, k_d constants that depend on the thermal capacity and conductivity of the fuel and coolant,

h_i instantaneous water level in the *i*th zone control compartment, cm

m_i constant,

q_i voltage signal given to the control valve of the *i*th zone, V

μ_f fuel reactivity coefficient, K-^{1}

μ_c coolant reactivity coefficient, K-^{1}

T_{f0} steady state value of the fuel temperature, K

T_{c0} steady state value of the coolant temperature, K

1 Chapter 1: Introduction

1.1 Background

A large Pressurized Heavy Water Reactor (PHWR) is a high order complex system with a large number of states and input variables. Designing an efficient and safe controller for such a system has been a research topic for a long time. Various models have been constructed and used to design controllers for a reactor. An accurate method that has been used in both the research community and industry is the nodal method. This method solves the neutron diffusion equation by dividing the reactor core into a number of zones or nodes such that the coupling of the zones is considered by the coupling coefficients defined in the model. In this thesis, a reactor nodal core model of a large 540 MWe (Megawatt electrical) PHWR is employed.

In the literature, different researchers have proposed various methods to reduce or decouple a sophisticated system in order to neglect the very slow modes of the system response or less coupled states of the system. These attempts have led to a number of system reduction and decoupling algorithms for complex systems. These methods have been used to design efficient controllers for complicated systems.

A brief review of the existing studies on both the reactor nodal core modeling and decoupling methods is presented in this section. The reactor nodal core model of the system is utilized during this thesis to measure the coupling between the states of the system and a decoupling algorithm is introduced to design optimal decentralized controllers for a large 540 MWe PHWR.

1.1.1 Reactor Nodal Core Model of a Large 540 MWe PHWR

Nodal methods are an accurate way of describing the behavior of a large nuclear reactor, like a large PHWR. A variety of nodal methods exist, all of which have the common goal of solving the neutron diffusion equation for averaged fluxes in homogenized zones [1]. The nodal model is based on the concept of coupled-core kinetics [2]. The reactor core is divided into divisions or nodes where the neutron flux and material composition are considered to be homogenous. These zones can then be considered as small cores and coupled through neutron diffusion. In this way, the model can be utilized for spatial control for a large nuclear reactor.

A spatial reactor nodal core model was developed by Tiwari [3], and the 540 MWe PHWR model [4], was used. The reactor core is comprised of 14 zones, 7 zones per axial half, each zone representing one node in the model. Each zone includes 5 state equations with the inclusion of the thermal-hydraulic reactivity feedbacks, thus making it a 72^{nd} order system. These states include the zonal iodine concentration, xenon concentration, delayed neutron precursors' concentration, liquid zone water level, power or neutron flux, fuel, and coolant temperatures. The liquid zone control compartments of a CANDU (CANada Deuterium Uranium) reactor can be seen in Fig. 1.1 which is identical to the large PHWR in India [5].

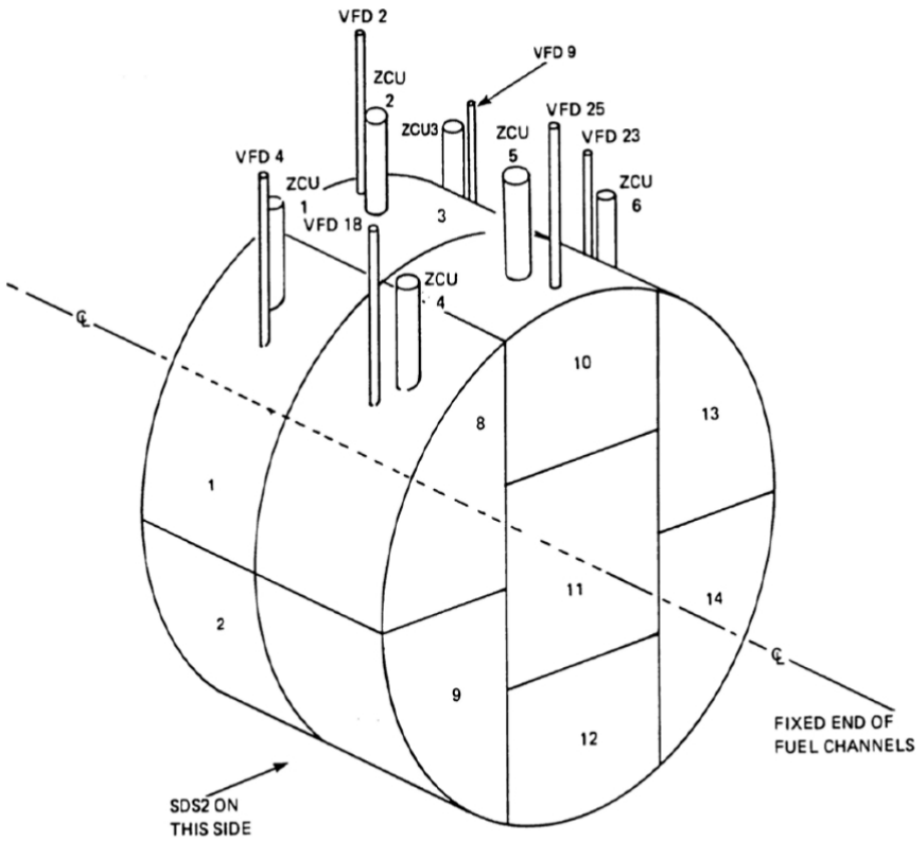

Figure 1.1: Liquid zonal control compartments of a CANDU reactor [6]

The large PHWR is a pressurized heavy water reactor that uses natural uranium oxide as fuel and heavy water as the moderator and coolant. Its power outputs are 1800 MW thermal power and 540 MW electrical power. The core dimensions are 800 cm diameter and 600 cm length. Due to its vastness in comparison to the neutron migration length, there is a need for reactivity devices distributed spatially and flux detecting mechanisms. To be able to control and observe the neutron flux distribution, the core has been divided into 14 zones. Each zone contains a Liquid Zone Controller (LZC) compartment which is used as the primary method of continuous fine control of the reactivity by varying the

light water levels. The higher the water level, the lower the reactivity insertion and the lower the reactor power will be in that particular zone and surrounding area. The lower the water level, the higher the reactivity insertion and the higher the reactor power will be in that particular zone and surrounding area. The main purpose of the liquid zone control system is to spatially control the power distribution while averting any xenon induced oscillation [7]. It also compensates for any small perturbations that cause small reactivity changes, such as the refueling process. It is sufficient to model the liquid zone control system to study the effects of the xenon induced spatial oscillations. The liquid zone control system provides a reactivity range of around $\pm$3.5 mk. This system is sufficient for the occurrences of regular reactivity perturbations. In the case of any unusual events that require an insertion of more than +3.5 mk, the adjuster rods system will be activated, and with less than -3.5 mk, the mechanical control rods system will be activated.

The reactor power can be detected and measured using the following devices. In each zone, there are 2 in-core vertical flux detectors that measure the zonal power. It measures the neutron flux at various points in the core for the estimation of power distribution and total power. There are three ex-core ion chambers that are used to measure the global power [3]. However, there exists no instrument that can measure the iodine, xenon, and delayed neutron precursors' concentrations which are pertinent in this system [8].

The 14 zones in the reactor are considered as small cores coupled through neutron diffusion. With the various neutron interactions like neutron production and absorption in

each zone and the leakage of neutrons among different zones, the rate of change of power in a zone can be given as [4]:

$$\frac{dP_i}{dt} = \frac{\left(\rho_{exi} + \rho_{fi} + \rho_{ci}\right) - \beta - \frac{\bar{\sigma}_{xi} X_i}{\Sigma_{ai}}}{l} P_i + \sum_{g=1}^{m_d} \left(\lambda_g C_{ig}\right) + \frac{1}{l} \sum_{j=1}^{N} \left(\alpha_{ji} P_j - \alpha_{ij} P_i\right) \tag{1.1}$$

The microscopic thermal neutron cross section of ^{135}Xe for each zone is given as:

$$\bar{\sigma}_{xi} = \frac{\sigma_{xi}}{E_{eff} \Sigma_{fi} \mathrm{V'}_i}; \qquad (i = 1, 2, \dots, N) \tag{1.2}$$

The accuracy of the nodal model depends highly on the coupling coefficients. They depend on the geometry, material composition, and distance between the zones. The degree of coupling among the zones is described as [9]:

$$\alpha_{ij} = \begin{cases} \dfrac{D v l \Psi_{\mathrm{ij}}}{d_{ij} V'_i} & if\ i \neq j \\ 0 & if\ i = j \end{cases} \tag{1.3}$$

Delayed neutron precursors occur by nuclear fission but are lost through radioactive decay. Since the dynamics of iodine and xenon are substantially slower than that of the precursors, only one effective group of delayed neutron precursors is considered, i.e. m_d = 1. Therefore, the delayed neutron precursors' concentration in different zones is given by [3]:

$$\frac{dC_{ig}}{dt} = \frac{\beta_g}{l} P_i - \lambda_g C_{ig}; \qquad (i = 1, 2, \dots N, g = 1, 2, \dots, m_d) \tag{1.4}$$

^{135}Xe is a significant fission product due to its extremely large thermal neutron absorption cross section, fairly large fission yield, and unstable nature. It is produced as a direct fission product and through the radioactive β-decay of ^{135}Te where the decay of ^{135}Te into ^{135}I is practically instantaneous [9, 10]:

$$^{135}\text{Te} \xrightarrow{<1\ min} {}^{135}\text{I} \rightarrow {}^{135}\text{Xe} \rightarrow {}^{135}\text{Cs} \rightarrow {}^{135}\text{Ba} \tag{1.5}$$

This xenon reactivity feedback causes changes in the neutron flux distribution and in turn causes spatial oscillations in the power distribution of a large thermal reactor.

The iodine and xenon concentrations in each zone can be represented as:

$$\frac{dI_i}{dt} = \gamma_I \Sigma_{fi} \mathrm{P}_i - \lambda_I I_i \tag{1.6}$$

$$\frac{dX_i}{dt} = \gamma_X \Sigma_{fi} \mathrm{P}_i + \lambda_I I_i - (\lambda_X + \bar{\sigma}_{xi} P_i) X_i \tag{1.7}$$

The rate of change of iodine concentration is defined as its rate of production through fission and its loss through radioactive decay. The rate of change of xenon concentration is defined as its rate of production through fission and iodine decay; its loss due to its radioactive decay and transformation of ^{135}Xe into stable ^{136}Xe [11].

The fuel and coolant temperature reactivity feedbacks have been considered for a more realistic modeling. The rates of change of fuel and coolant temperatures are described as:

$$\frac{dT_f}{dt} = k_a P_g - k_b (T_f - T_c) \tag{1.8}$$

$$\frac{dT_c}{dt} = k_c (T_f - T_c) - k_d (T_c - T_1) \tag{1.9}$$

The instantaneous rate of change of a ZCC (zonal control compartment) is directly proportional to the net flow rate of water in the ZCC. The variation of inflow of water to each zone is associated with the direct position of the control valve and the outflow is kept constant. The change in water level in each zone can be given as a function of input signals to the control valves and is described as:

$$\frac{dh_i}{dt} = -m_i q_i \tag{1.10}$$

The reactivity due to the control mechanism of the LZC that is directly proportional to the water level in the ZCC in its respected zone is defined as:

$$\rho_{exi} = -K_i^{'}(h_i - h_{i0}); \qquad (i = 1,2, \dots N) \tag{1.11}$$

Substituting the value of h_i from equation (1.11) in equation (1.1), it becomes:

$$\frac{dP_i}{dt} = \frac{-K'_i h_i - \beta - \frac{\bar{\sigma}_{xi} X_i}{\Sigma_{ai}}}{l} P_i + \sum_{g=1}^{m_d} (\lambda_g C_{ig}) + \frac{1}{l} \sum_{j=1}^{N} (\alpha_{ji} P_j - \alpha_{ij} P_i) \tag{1.12}$$

The variations in reactivity due to the fuel and coolant temperature are assumed to not change appreciably over normal control related transients and thus these changes are almost linear and can be defined as [3]:

$$\rho_{fi} = \mu_{fi}(T_f - T_{f0}) = \mu_{fi} \delta T_f \tag{1.13}$$

$$\rho_{ci} = \mu_{ci}(T_c - T_{c0}) = \mu_{ci} \delta T_c \tag{1.14}$$

The physical data of the reactor are given in Tables 1.1 and 1.2 [4].

Zone Number	Power (MW)	Volume (m^3)
1, 6, 8, 13	132.75	14.7
2, 7, 9, 14	135.99	14.7
3, 10	123.30	17.6
4, 11	98.55	8.8
5, 12	123.30	17.6

Table 1.1: Steady-state zone power levels and volumes

$l = 7.9\ x\ 10^{-4}\ s$	$m_d = 1$
$\lambda = 9.1\ x\ 10^{-2}\ s^{-1}$	$m_i = 2$
$\Sigma_f = 1.262\ x\ 10^{-3}\ cm^{-1}$	$K'_i = -3.5\ x\ 10^{-5}$
$\sigma_x = 1.2\ x\ 10^{-18}\ cm^2$	$h_{i0} = 100.0\ cm$
$\upsilon = 3.19\ x\ 10^5\ cm/s$	$T_{f0} = 547.2831°K$
$\gamma_I = 6.18\ x\ 10^{-2}$	$T_{c0} = 541.4037\ °K$
$\lambda_x = 2.1\ x\ 10^{-5}\ s^{-1}$	$T_1 = 539\ °K$
$\beta = 7.5\ x\ 10^{-3}$	$\mu_f = -3.4722\ x\ 10^{-6}/K$
$\Sigma_a = 3.2341\ x\ 10^{-3}\ cm^{-1}$	$\mu_f = 3.33333\ x\ 10^{-5}/K$
$E_{eff} = 3.2\ x\ 10^{-17}\ MJ$	$k_a = 1.38428\ x\ 10^{-3}\ K/J$
$\gamma_x = 6\ x\ 10^{-3}$	$k_b = 4.238\ x\ 10^{-1}\ s^{-1}$
$D = 0.9328\ cm$	$k_c = 1.758\ x\ 10^{-2}\ s^{-1}$
$\lambda_I = 2.878\ x\ 10^{-5}\ s^{-1}$	$k_d = 4.3016759\ x\ 10^{-2}\ s^{-1}$

Table 1.2: Physical data for the 540 MWe PHWR for all zones

1.1.2 Model Reduction

It is challenging to deal with higher order systems in controller design. Therefore, a reduced model is more manageable. The present work introduces an innovative approach to reduce the model by using a new decoupling algorithm. This method decouples the system by dividing the states into partitions by having the most dependent states in the

same partition. These partitions are then used for the design of sub-controllers thus creating decentralized controllers.

Decentralized controllers have gained more attention in both the nuclear industry and research communities throughout the last few decades. Since this structure has been proven to be more reliable, cost effective, and easily maintainable, attempts have been launched to practically apply it in nuclear power plants, e.g. in Taiwan [12]. However, dividing the controller into several sub-controllers would raise a few concerns that can be classified into two major groups: (a) selection of the system states that are controlled in a sub-controller and, (b) integration and communication of different sub-controllers to control the system as a whole.

In order to solve the former issue, various model reduction methods have been introduced. For example, Krylov spaces have been used to reduce the system and estimate it arbitrarily and precisely while maintaining the important properties of the system such as stability and controllability [13]. Generally, model reduction methods can be divided into three categories. The first category is called the continued fraction expansion that is based on obtaining a reduced model which matches some time moments and Markov parameters of the original model. For systems that can be estimated by low-pass filters, it can be shown that the continued fraction expansion of the Cauer second form is equivalent to matching time moments with a Taylor series expanding about $s = 0$. On the other hand, for the systems that can be estimated by high-pass filters, the Cauer first form is equivalent to matching Markov parameters with a Taylor series expanding

about $s = \infty$. The drawback of this reduction method is that it does not guarantee the stability of the reduced model even if the original model is stable. In the second category, called dominant mode, Davison suggested a method based on neglecting the eigenvalues of the system that are farther from the origin and retaining the dominant eigenvalues that estimate the system behavior more precisely [14]. However, the reduced model by Davison's method fails to maintain the accurate steady-state gains due to neglecting the contribution of eliminated eigenvalues. The third category is called optimum fitting that tries to minimize an error function defined based on the deviation of the reduced model response from a set of given sample data of the original system either in time-domain or frequency-domain [15]. However, the abovementioned algorithms try to estimate the system by a lower dimensional model instead of dividing it into several coupled sub-systems that can be safely controlled separately. On the other hand, a decentralized controller necessitates an algorithm that can introduce various sub-controllers that are as decoupled as possible.

In the literature, researchers have studied the problem of sensitivity and decoupling of the linearized systems in the last four decades. For example, in [16], Hautus and Heymann formalized a decoupling problem for linear systems employing a suitable compensator. The problem of data sensitivity and decoupling is formulated and solved in [17] and the necessary and sufficient conditions of the stability of the decoupled system are also presented. In 1976, for an *m*-input-*m*-output linear time-invariant system, the decoupling and data sensitivity problem was solved using an algebraic approach [18]. Nevertheless, the problem of distributing a controller, sensitivity, and decoupling of the states of the

system is of concern and has not been studied for state-space controllers to the knowledge of the author.

On the other hand, different methods in mathematics have been utilized to classify a set of data points such as fuzzy and hard clustering methods. Clustering is defined as partitioning a collection of unlabeled data into a number of groups or clusters such that data points that are more similar are put into one cluster [19]. Hard clustering algorithms assigned each data point to one and only one of the partitions, assuming well defined boundaries between the clusters. However, the boundaries between the clusters may not be clearly definable, the fuzzy environment of decision making would then be an appropriate tool to tackle the clustering problem, e.g. Fuzzy C-Means Clustering algorithm and Fuzzy Mountain Clustering. The problem of finding the optimal fuzzy clustering can be formulated as minimizing an objective function subject to conditions on membership functions. Fuzzy C-Means Clustering algorithm is based on the fuzzy-equivalent of the nearest mean hard clustering algorithm. This objective function is defined considering the sum of squared errors of data points with respect to the centers of partitions [20].

There have been methods that reduce the dimensionality of high-order systems, such as Principal Components Algorithm (PCA) [21]. This method's reduction is based on performing a covariance analysis between factors. The data taken can be plotted in multi-dimensional space producing a cloud. The trends are characterized by extracting directions where a cloud is more extended. The directions taken produce components

whereby reducing the multi-dimensional cloud. However, this method is mainly useful when wanting to discover unknown trends in a dataset. Therefore, in systems where these trends are already known based on previous studies, this method is not useful.

Another type of reduction technique used in decoupling methods is dynamic decoupling. These methods are used in systems that undergo drastic changes in its dynamic behaviour causing excitations. Therefore, these methods are not useful in systems that do not fluctuate very far from its steady-state point. There are various methods that exist, each with their own objectives based on the dynamics of the system, for example, a dynamic decoupling method was proposed by Mikloslovic and Gao to control complex uncertain systems [22].

1.2 Motivation of Thesis

A large PHWR is a high order complex system with a large number of states and input variables. Reduction algorithms have already been used to reduce the order of this system to design controllers. However, they neglect the states in the system that may have major impacts on the system behavior in different situations. In this thesis, a decoupling algorithm is introduced using state-space representation of the system that reduces the coupling between the states of the system and at the same time keeps all the states of the system in the control loop.

1.3 Objectives of Thesis

1. Design and test a decoupling algorithm using the notion of sensitivity of the states with respect to each other.
2. Implement the decoupling algorithm to a large PHWR and partition the system.
3. Design optimal decentralized controllers for the sub-systems and compare the results to an optimal centralized controller.

1.4 Organization of Thesis

In chapter 1, an introduction to the research and background is given with the motivation and objectives of the thesis. In chapter 2, the state-space control theory, its application to this thesis, and the optimal control theory is given. In chapter 3, the design of the decoupling algorithm is given with the sensitivity definition, the decoupling criteria, the objective function, the steps of the algorithm, and the construction of the sub-systems. In chapter 4, the simulation results of the partitions are given, the centralized and decentralized controllers are discussed and analyzed, and a fail-safe study of the controllers is shown. In chapter 5, a conclusion of the findings for this research and future work recommendations is given.

2 Chapter 2: State-Space Control

2.1 Linear Time-Invariant Systems with Input

A linear time-invariant system with input and output can be identified by:

$$\dot{\boldsymbol{z}}(t) = A\boldsymbol{z}(t) + B\boldsymbol{u}(t) \tag{2.1}$$

$$\boldsymbol{z}(0) = \boldsymbol{z}_0 \tag{2.2}$$

$$\boldsymbol{y}(t) = C\boldsymbol{z}(t) + D\boldsymbol{u}(t) \tag{2.3}$$

where $\boldsymbol{z}(t)$ is a vector including all of the system states as functions of time, $\boldsymbol{u}(t)$ and $\boldsymbol{y}(t)$ are the input (or the feedback of a controller) and the output of the system, respectively, where both are functions of time. *A, B, C,* and *D* are time-invariant matrices that define the behaviour of a linear or non-linear system around an equilibrium point. The matrix *D* is usually considered as a zero matrix.

Therefore, the solution to this system of equations can be immediately obtained by:

$$\boldsymbol{y}(t) = Ce^{At}\boldsymbol{z}_0 + \int_0^t Ce^{A(t-s)}B\boldsymbol{u}(s)ds \tag{2.4}$$

where e^X is the exponential of matrix *X* and can be defined as:

$$e^X := \sum_{n=0}^{\infty} \frac{X^n}{n!} \tag{2.5}$$

where X^0 is defined to be the identity matrix.

2.1.1 Linearization of a Non-Linear System

A general non-linear system can be represented by the following equations:

$$\dot{\boldsymbol{x}} = f(\boldsymbol{x}, \boldsymbol{u}) \qquad f: \boldsymbol{R}^n \times \boldsymbol{R}^m \to \boldsymbol{R}^n \tag{2.6}$$

$$\boldsymbol{y} = h(\boldsymbol{x}, \boldsymbol{u}) \qquad h: \boldsymbol{R}^n \times \boldsymbol{R}^m \to \boldsymbol{R}^p \tag{2.7}$$

where $\boldsymbol{x}(n \times 1)$ is the state vector of the system, $\boldsymbol{u}(m \times 1)$ is the control input to the system, $\dot{\boldsymbol{x}}(n \times 1)$ is the rate of change of the states in time and $\boldsymbol{y}(p \times 1)$ is the output of the system.

Assume that $\overline{\boldsymbol{x}}$ is an equilibrium point and for $\boldsymbol{u} = \overline{\boldsymbol{u}}$, the non-linear system can be approximated by the Taylor series as:

$$f(\boldsymbol{x}, \boldsymbol{u}) \approx \left[\frac{\partial f}{\partial \boldsymbol{x}}(\overline{\boldsymbol{x}}, \overline{\boldsymbol{u}})\right](\boldsymbol{x} - \overline{\boldsymbol{x}}) + \left[\frac{\partial f}{\partial \boldsymbol{u}}(\overline{\boldsymbol{x}}, \overline{\boldsymbol{u}})\right](\boldsymbol{u} - \overline{\boldsymbol{u}}) \tag{2.8}$$

$$h(\boldsymbol{x}, \boldsymbol{u}) \approx h(\overline{\boldsymbol{x}}, \overline{\boldsymbol{u}}) + \left[\frac{\partial h}{\partial \boldsymbol{x}}(\overline{\boldsymbol{x}}, \overline{\boldsymbol{u}})\right](\boldsymbol{x} - \overline{\boldsymbol{x}}) + \left[\frac{\partial h}{\partial \boldsymbol{u}}(\overline{\boldsymbol{x}}, \overline{\boldsymbol{u}})\right](\boldsymbol{u} - \overline{\boldsymbol{u}}) \tag{2.9}$$

If $\tilde{\boldsymbol{x}} = (\boldsymbol{x} - \overline{\boldsymbol{x}})$, $\tilde{\boldsymbol{u}} = (\boldsymbol{u} - \overline{\boldsymbol{u}})$, and $\tilde{\boldsymbol{y}} = (\boldsymbol{y} - h(\overline{\boldsymbol{x}}, \overline{\boldsymbol{u}}))$, then, the linear approximation of the system around $\overline{\boldsymbol{x}}$ and $\overline{\boldsymbol{u}}$ can be shown by:

$$\dot{\tilde{\boldsymbol{x}}} = A\tilde{\boldsymbol{x}} + B\tilde{\boldsymbol{u}} \tag{2.10}$$

$$\tilde{\boldsymbol{y}} = C\tilde{\boldsymbol{x}} + D\tilde{\boldsymbol{u}} \tag{2.11}$$

where $A = \left[\frac{\partial f}{\partial x}(\overline{\boldsymbol{x}}, \overline{\boldsymbol{u}})\right]$, $B = \left[\frac{\partial f}{\partial \boldsymbol{u}}(\overline{\boldsymbol{x}}, \overline{\boldsymbol{u}})\right]$, $C = \left[\frac{\partial h}{\partial x}(\overline{\boldsymbol{x}}, \overline{\boldsymbol{u}})\right]$ and $D = \left[\frac{\partial h}{\partial \boldsymbol{u}}(\overline{\boldsymbol{x}}, \overline{\boldsymbol{u}})\right]$.

2.1.2 Linearization of a Large PHWR

A large PHWR that was represented by equations (1.1) to (1.13) should be linearized in order to describe the behavior of the reactor in the area of the steady-state operating point due to any minor change in power, delayed precursors' concentration, iodine, xenon concentration, liquid zone water levels, fuel and coolant temperatures [4]. The global reactor power P_g is considered to be constant, when operating at steady state, hence the power distribution does not vary in time. This condition can be accomplished when the zonal power levels are constant and the delayed neutron precursors', iodine, and xenon concentrations are in equilibrium with them. From the nodal equations (1.4), (1.6), (1.7), (1.10), and (1.12) the following steady state condition can be attained:

$$C_{i0} = \frac{\beta P_{i0}}{\lambda l}\ ; \tag{2.12}$$

$$I_{i0} = \frac{\gamma_I \Sigma_{fi} P_{i0}}{\lambda_I}; \tag{2.13}$$

$$X_{i0} = \frac{(\gamma_X + \gamma_I)\Sigma_{fi} P_{i0}}{\lambda_X + \bar{\sigma}_{Xi} P_{i0}}; \tag{2.14}$$

$$h_{i0} = \frac{\bar{\sigma}_{Xi} X_{i0}}{K'_i \Sigma_{\mathrm{ai}}}. \tag{2.15}$$

Using these steady state values in equation (1.12) and setting $\frac{dP_i}{dt} = 0$, the steady-state power distribution can be calculated based on the following equations:

$$-\alpha_{ii} P_{i0} + \sum_{j=1}^{N} \alpha_{ij} P_{j0} = 0; \quad i = 1,2 \ldots N, \tag{2.16}$$

$$P_{g0} = \sum_{i=1}^{N} P_{i0} \tag{2.17}$$

The steady-state zonal power levels can be obtained for a corresponding global power, P_{g0}, by solving the above equations.

Considering an increment δq_i, for the i^{th} input variable, the resulting zonal change of the states of the system, power levels, delayed precursor, iodine, and xenon concentrations, ZCC water levels, fuel and coolant temperatures, can be shown by δP_i, δC_i, δI_i, δX_i. δh_i, δT_f, and δT_c, respectively.

$$q_i = q_{i0} + \delta q_i \tag{2.18}$$

$$P_i = P_{i0} + \delta P_i \tag{2.19}$$

$$C_i = C_{i0} + \delta C_i \tag{2.20}$$

$$I_i = I_{i0} + \delta I_i \tag{2.21}$$

$$X_i = X_{i0} + \delta X_i \tag{2.22}$$

$$h_i = h_{i0} + \delta h_i \tag{2.23}$$

Hence, the new state space variables can be introduced by:

$$z_I = \left[\frac{\delta I_1}{I_{10}} \frac{\delta I_2}{I_{20}} \frac{\delta I_3}{I_{30}} \quad \dots \quad \frac{\delta I_N}{I_{N0}}\right]^T \tag{2.24}$$

$$z_X = \left[\frac{\delta X_1}{X_{10}} \frac{\delta X_2}{X_{20}} \frac{\delta X_3}{X_{30}} \quad \dots \quad \frac{\delta X_N}{X_{N0}}\right]^T \tag{2.25}$$

$$z_C = \left[\frac{\delta C_1}{C_{10}} \frac{\delta C_2}{C_{20}} \frac{\delta C_3}{C_{30}} \quad \dots \quad \frac{\delta C_N}{C_{N0}}\right]^T \tag{2.26}$$

$$z_H = [\delta h_1 \delta h_2 \delta h_3 \quad \dots \quad \delta h_N]^T \tag{2.27}$$

$$z_P = \left[\frac{\delta P_1}{P_{10}} \frac{\delta P_2}{P_{20}} \frac{\delta P_3}{P_{30}} \quad \dots \quad \frac{\delta P_N}{P_{N0}}\right]^T \tag{2.28}$$

$$z_{T_f} = \delta T_f \tag{2.29}$$

$$z_{T_c} = \delta T_c \tag{2.30}$$

Therefore, the new state, control, and output vectors can be defined as:

$$\boldsymbol{z} = \left[\boldsymbol{z}_I^T \boldsymbol{z}_X^T \boldsymbol{z}_C^T \boldsymbol{z}_H^T \boldsymbol{z}_P^T \boldsymbol{z}_{T_f}^T \boldsymbol{z}_{T_c}^T\right]^T \tag{2.31}$$

$$\boldsymbol{u} = [\delta q_1 \delta q_2 \delta q_3 \quad \dots \quad \delta q_N]^T \tag{2.32}$$

$$\boldsymbol{y} = \boldsymbol{z}_P \tag{2.33}$$

The non-linear equations of the reactor can be linearized around the steady state point based on the following equations:

$$\frac{d}{dt}\left(\frac{\delta P_i}{P_{i0}}\right) = -\frac{1}{l}\left(\beta + \sum_{j=1}^{N} \alpha_{ij} \frac{P_{j0}}{P_{i0}}\right)\frac{\delta P_i}{P_{i0}} + \frac{1}{l}\sum_{j=1}^{N} \alpha_{ij} \frac{P_{j0}}{P_{i0}} \frac{\delta P_j}{P_{j0}} + \frac{\beta}{l}\frac{\delta C_{ik}}{C_{ik0}} - \frac{\bar{\sigma}_{xi} X_{i0}}{l\Sigma_{ai}}\frac{\delta X_i}{X_{i0}} \tag{2.34}$$

$$-\frac{K'_i}{l}\delta h_i + \frac{\mu_{fi}\delta T_f}{l} + \frac{\mu_{ci}\delta T_c}{l}$$

$$\frac{d}{dt}\left(\frac{\delta C_{ik}}{C_{ik0}}\right) = \lambda_k \frac{\delta P_i}{P_{i0}} - \lambda_k \frac{\delta C_{ik}}{C_{ik0}} \tag{2.35}$$

$$\frac{d}{dt}\left(\frac{\delta I_i}{I_{i0}}\right) = \lambda_I \frac{\delta P_i}{P_{i0}} - \lambda_k \frac{\delta I_i}{I_{i0}} \tag{2.36}$$

$$\frac{d}{dt}\left(\frac{\delta X_i}{X_{i0}}\right) = \left(\lambda_X - \lambda_I \frac{I_{i0}}{X_{i0}}\right)\frac{\delta P_i}{P_{i0}} + \lambda_I \frac{I_{i0}}{X_{i0}}\frac{\delta I_i}{I_{i0}} - (\lambda_x + \bar{\sigma}_{xi} P_{i0})\frac{\delta X_i}{X_{i0}} \tag{2.37}$$

$$\frac{d\delta h_i}{dt} = -m_i \delta q_i \tag{2.38}$$

$$\frac{d(\delta T_f)}{dt} = k_a \sum_{i=1}^{N} \delta P_i - k_b \delta T_f + k_b \delta T_c \tag{2.39}$$

$$\frac{d(\delta T_c)}{dt} = k_c \delta T_f - (k_c + k_d)\delta T_c \tag{2.40}$$

The above equations can be written in the standard state space representation of a linear time-invariant system as:

$$\dot{\boldsymbol{z}} = A\boldsymbol{z} + B\boldsymbol{u} \tag{2.41}$$

$$\boldsymbol{y} = C\boldsymbol{z} \tag{2.42}$$

Matrices *A*, *B*, and *C* are given as:

$$A = \begin{bmatrix} A_{II} & A_{IX} & A_{IC} & A_{IH} & A_{IP} & A_{IT_f} & A_{IT_c} \\ A_{XI} & A_{XX} & A_{XC} & A_{XH} & A_{XP} & A_{XT_f} & A_{XT_c} \\ A_{CI} & A_{CX} & A_{CC} & A_{CH} & A_{CP} & A_{CT_f} & A_{CT_c} \\ A_{HI} & A_{HX} & A_{HC} & A_{HH} & A_{HP} & A_{HT_f} & A_{HT_c} \\ A_{PI} & A_{PX} & A_{PC} & A_{PH} & A_{PP} & A_{PT_f} & A_{PT_c} \\ A_{T_fI} & A_{T_fX} & A_{T_fC} & A_{T_fH} & A_{T_fP} & A_{T_fT_f} & A_{T_fT_c} \\ A_{T_cI} & A_{T_cX} & A_{T_cC} & A_{T_cH} & A_{T_cP} & A_{T_cT_f} & A_{T_cT_c} \end{bmatrix} \tag{2.43}$$

$$B = \begin{bmatrix} B_I^T & B_X^T & B_C^T & B_H^T & B_P^T & B_{T_f}^T & B_{T_c}^T \end{bmatrix}^T \tag{2.44}$$

$$C = \begin{bmatrix} C_I & C_X & C_C & C_H & C_P & C_{T_f} & C_{T_c} \end{bmatrix} \tag{2.45}$$

The abovementioned sub matrices of the system can be listed as follows:

$$A_{II} = diag.-\lambda_I Id_N \tag{2.46}$$

$$A_{IX} = 0 \tag{2.47}$$

$$A_{IC} = 0 \tag{2.48}$$

$$A_{IH} = 0 \tag{2.49}$$

$$A_{IP} = \lambda_I Id_N \tag{2.50}$$

$$A_{IT_f} = 0 \tag{2.51}$$

$$A_{IT_c} = 0 \tag{2.52}$$

$$A_{XI} = \lambda_I diag.\left[\frac{I_{10}}{X_{10}} \dots \frac{I_{N0}}{X_{N0}}\right] \tag{2.53}$$

$$A_{XX} = diag.\left[(-\lambda_X + \bar{\bar{\sigma}}_{X1}P_{10}) \dots (-\lambda_X + \bar{\bar{\sigma}}_{XN}P_{N0})\right] \tag{2.54}$$

$$A_{XC} = 0 \tag{2.55}$$

$$A_{XH} = 0 \tag{2.56}$$

$$A_{XP} = diag.\left[\left(\lambda_X - \lambda_I \frac{I_{10}}{X_{10}}\right) \dots \left(\lambda_X - \lambda_I \frac{I_{N0}}{X_{N0}}\right)\right] \tag{2.57}$$

$$A_{XT_f} = 0 \tag{2.58}$$

$$A_{XT_c} = 0 \tag{2.59}$$

$$A_{CI} = 0 \tag{2.60}$$

$$A_{CX} = 0 \tag{2.61}$$

$$A_{CC} = -\lambda Id_N \tag{2.62}$$

$$A_{CH} = 0 \tag{2.63}$$

$$A_{CP} = \lambda Id_N \tag{2.64}$$

$$A_{CT_f} = 0 \tag{2.65}$$

$$A_{CT_c} = 0 \tag{2.66}$$

$$A_{HI} = 0 \tag{2.67}$$

$$A_{HX} = 0 \tag{2.68}$$

$$A_{HC} = 0 \tag{2.69}$$

$$A_{HH} = 0 \tag{2.70}$$

$$A_{HP} = 0 \tag{2.71}$$

$$A_{HT_f} = 0 \tag{2.72}$$

$$A_{HT_c} = 0 \tag{2.73}$$

$$A_{PI} = 0 \tag{2.74}$$

$$A_{PX} = diag.\left[-\left(\frac{\bar{\sigma}_{X1}X_{10}}{l\Sigma_{a1}}\right) \dots -\left(\frac{\bar{\sigma}_{XN}X_{N0}}{l\Sigma_{aN}}\right)\right] \tag{2.75}$$

$$A_{PC} = \frac{\beta}{l} Id_N \tag{2.76}$$

$$A_{PH} = -\frac{K'_i}{l} Id_N \tag{2.77}$$

$$A_{PP}(i,j) = \begin{cases} -\frac{1}{l}\left(\beta + \left(\sum_{j=1}^{N} \alpha_{ij}\frac{P_{j0}}{P_{i0}}\right) - \alpha_{ii}\right) & if\ i = j \\ \frac{1}{l}\alpha_{ij}\frac{P_{j0}}{P_{io}} & if\ i \neq j \end{cases} \tag{2.78}$$

$$A_{PT_f} = \frac{\mu_f}{l}\begin{bmatrix}1\\ \vdots \\ 1\end{bmatrix}\Bigg\} N - times \tag{2.79}$$

$$A_{PT_c} = \frac{\mu_c}{l}\begin{bmatrix}1\\ \vdots \\ 1\end{bmatrix}\Bigg\} N - times \tag{2.80}$$

$$A_{T_fI} = 0 \tag{2.81}$$

$$A_{T_fX} = 0 \tag{2.82}$$

$$A_{T_fC} = 0 \tag{2.83}$$

$$A_{T_fH} = 0 \tag{2.84}$$

$$A_{T_fP} = k_a[P_{10} \dots P_{N0}] \tag{2.85}$$

$$A_{T_fT_f} = -k_b \tag{2.86}$$

$$A_{T_fT_c} = k_b \tag{2.87}$$

$$A_{T_cI} = 0 \tag{2.88}$$

$$A_{T_cX} = 0 \tag{2.89}$$

$$A_{T_cC} = 0 \tag{2.90}$$

$$A_{T_cH} = 0 \tag{2.91}$$

$$A_{T_cP} = 0 \tag{2.92}$$

$$A_{T_cT_f} = k_c \tag{2.93}$$

$$A_{T_cT_c} = -(k_c + k_d) \tag{2.94}$$

$$B_I = 0 \tag{2.95}$$

$$B_X = 0 \tag{2.96}$$

$$B_C = 0 \tag{2.97}$$

$$B_H = -m_i Id_N \tag{2.98}$$

$$B_P = 0 \tag{2.99}$$

$$B_{T_f} = 0 \tag{2.100}$$

$$B_{T_c} = 0 \tag{2.101}$$

$$C_I = 0 \tag{2.102}$$

$$C_X = 0 \tag{2.103}$$

$$C_C = 0 \tag{2.104}$$

$$C_H = 0 \tag{2.105}$$

$$C_P = Id_N \tag{2.106}$$

$$C_{T_f} = 0 \tag{2.107}$$

$$C_{T_c} = 0 \tag{2.108}$$

where Id_N is the identity matrix of dimension N and $diag.(a_1 \ldots a_n)$ is the diagonal n x n matrix with $a_1 \ldots a_n$ being the diagonal elements.

2.2 Controllability

Considering a linear-time-invariant system, (*A*,*B*), the notion of controllability can be defined as the ability of the system to reach all its possible states, which is usually in $\boldsymbol{R}^n$, for finite control input in finite time. In other words, for any possible state of the system there exists at least a control input defined on [0,*t*] that can take the system from an initial point to the final state. Therefore, if all the states of system are reachable, (*A*,*B*) is called *controllable*. In order to check the controllability of a system, it can be shown that the rank of the following *n* x *nm* matrix should be *n*, which is the number of the system states.

$$Q_c = [B\ AB\ A^2B \dots A^{n-1}B] \tag{2.109}$$

This matrix is called the *controllability matrix*. If this rank is less than *n*, the system can be divided into controllable and uncontrollable subsystems by Kalman Decomposition algorithm. If the uncontrollable eigenvalues are all in the open left hand complex plane, then the system is at least stabilizable. That means that the system can approach any state but the closed-loop eigenvalues cannot be arbitrarily assigned.

Controllability of a Large PHWR

In order to control a reactor, first the controllability of the system in (2.41) should be checked. It can be shown that for a 540 MWe large PHWR using the nodal model, the assigned controllability matrix is of rank *n* and the system is fully controllable [23]. This indicates that the zonal power levels can be controlled by the variation of water levels in

the zones, independently. Hence, by a specific control input, the power distribution in a reactor can be controlled.

However, in the case of distributing the controller, where sub-systems are considered, the controllability of each sub-system should also be checked before designing a controller.

2.3 Observability

Another system property, just as important as controllability, is observability. It is important to know whether you can estimate all the system states using the measured output and input signal. In the real world, measuring all the system states at each instant is not feasible. Therefore, if the system (*C*,*A*) is observable, then an observer can be designed to estimate the states. It can be shown that a system is observable if and only if the following *n* x *np* matrix (*observability matrix*) is of rank *n*.

$$Q_o = [C \quad CA \quad \dots \quad CA^{n-1}]^T \tag{2.110}$$

The estimated state equations of the system can be written as:

$$\dot{\hat{\boldsymbol{z}}} = A\hat{\boldsymbol{z}} + B\boldsymbol{u} + L(\boldsymbol{y} - \widehat{\boldsymbol{y}}),\ \hat{\boldsymbol{z}}(0) = \hat{\hat{\boldsymbol{z}}}_0 \tag{2.111}$$

$$\widehat{\boldsymbol{y}} = C\hat{\boldsymbol{z}} \tag{2.112}$$

If there exists an *n* x *p* matrix *L* such that all the eigenvalues of *A*-*LC* lie on the left half complex plane, then (*C*,*A*) is observable and *L* is called the full state observer of the system.

Observability of a Large PHWR

Observability of a reactor is also a vital property of the system since all of the system states should be fed back to the controller. Therefore, they must be estimated knowing the measured states of the system. It can be shown that the linearized model of the 540 MWe PHWR is fully observable [23] and a matrix *L* can be optimally designed as the observer of the system.

2.4 Optimal Control

An optimal control problem can be stated as follows:

Find a control law $u = \phi(t)$ that is in the class of admissible controls (ϕ is continuous, stabilizing, and results in a unique closed-loop solution) and minimizes the following cost function:

$$J(\boldsymbol{z}_0, \phi) = \int_0^\infty [\boldsymbol{z}^T(t) Q \boldsymbol{z}(t) + \phi^T(t)\, R \phi(t)] dt \tag{2.113}$$

where *Q* is a symmetric positive semi-definite matrix and *R* is a symmetric positive definite matrix. Since *Q* is positive semi-definite, $\boldsymbol{z}^T(t) Q \boldsymbol{z}(t) \geq 0$ represents the penalty incurred at time *t* for state trajectories that deviate from 0. Similarly, *R* is positive definite, hence $\phi^T(t) R \phi(t) > 0$ represents the control effort at time *t* in order to regulate $\boldsymbol{z}(t)$ to 0.

It can be shown that a solution to this problem is in matrix quadratic form. Therefore, equation (2.113) results in the following matrix quadratic equation, called the algebraic Riccati equation:

$$A^T P + PA - PB - R^{-1}B^T P + Q = 0 \quad (2.114)$$

This equation should be solved for P in order to find the minimizing control law given by:

$$\boldsymbol{u} = -R^{-1}B^T P\boldsymbol{z} \quad (2.115)$$

and the optimal state feedback gain K can be expressed as:

$$K = -R^{-1}B^T P \quad (2.116)$$

Therefore, the closed-loop system equation is stated as:

$$\dot{\boldsymbol{z}} = (A + BK)\boldsymbol{z} \quad (2.117)$$

Based on the duality theorem in state-space control, finding an observer for (C,A) is equivalent to finding a controller for (A^T,C^T). Therefore, it is natural to introduce the notion of the optimal observer according to the linear quadratic optimal control law. Hence, an optimal observer, L, can be designed considering L^T as the optimal feedback law for (A^T,C^T) as the dual controller to (C,A).

Optimal Control of a Large PHWR

A control design methodology should be utilized to produce controllers with the desired objectives. A cost criterion is formulated based on these objectives. The optimal control law solves the optimization problem based on the minimization of the given cost criterion. In this way, controllers of the reactor can be optimally designed for the system.

3 Chapter 3: Decoupling Algorithm

The complexity of a large system can result in difficulties in controller design that gives rise to the concept of model reduction in order to facilitate the design process. In model reduction methods, the dominant features of the system are studied and the rest of the states of the system are neglected. In the case of controlling a large PHWR, due to its safety-critical nature, neglecting the system features can be risky. Therefore, decoupling algorithms are needed to reduce the model without losing the dominant characteristics of the system. A number of decoupling algorithms have been suggested in the literature to study the sensitivity of linearized systems. However, in order to design a decentralized control system, the sensitivity of state variables of a linear system should be investigated and the most coupled states should be grouped together. This chapter presents a systematic decoupling algorithm for a linear time-invariant system without input to partition the system and consequently divide an optimal centralized controller to a number of sub-controllers that can separately control the partitions of the system. For this purpose, the notion of sensitivity of a state with respect to other states is defined. Subsequently, by mimicking the clustering algorithms, an objective function is introduced to find the most decoupled and evenly distributed partitioning. This algorithm has been applied to the reactor nodal core model of a large PHWR to design decentralized controllers. The results have been presented and discussed in the next chapter.

3.1 Sensitivity

Definition (Sensitivity): In general, in system engineering, sensitivity of a parameter X of a system with respect to parameter Y at equilibrium is the rate of change of X with respect to Y after a small amount of time when parameter Y is disturbed by a small change, namely $\Delta > 0$. In a linear time-invariant (LTI) system, the sensitivity of state z_i with respect to z_j while z_j is perturbed by δz_j after τ seconds can be defined as,

$$S(\tau) = \left|\frac{\partial z_i}{\partial z_j}(\tau)\right| = \left|\frac{\dot{z}_i(\tau)}{\dot{z}_j(\tau)}\right| \tag{3.1}$$

The linear system without input variables should be considered to determine the sensitivity of different states with respect to each other. The reasons for this is that this algorithm is utilized to design a controller for the system and thus has no input to the system; in order to design controllers for a system, the intrinsic behaviour of the system must be studied which is done through the sensitivity analysis; and since there is no coupling between the input states and any of the other states, these states must be pushed somehow. Therefore, the following system of ordinary differential equations needs to be solved to calculate $\dot{z}_i(\tau)$:

$$\dot{\boldsymbol{z}}(t) = A\boldsymbol{z}(t) \tag{3.2}$$

$$\boldsymbol{z}(0) = \boldsymbol{z}_0^j = (0, 0, \dots, \delta z_j, 0, \dots, 0)^T \tag{3.3}$$

where $\boldsymbol{z}_0^j$ is the initial condition of the differential equation when z_j is perturbed by δz_j.

The solution of $\boldsymbol{z}$ at time t is:

$$\boldsymbol{z}(t) = e^{At}{\boldsymbol{z}_0}^j \tag{3.4}$$

Therefore, based on (3.2), $\dot{\boldsymbol{z}}$ after τ seconds is:

$$\dot{\boldsymbol{z}}(\tau) = Ae^{A\tau}{\boldsymbol{z}_0}^j \tag{3.5}$$

By substituting (3.3) in (3.5), sensitivity of state z_i with respect to z_j at time τ can be formulated as:

$$S(\tau) = \left|\frac{\dot{z}_i(\tau)}{\dot{z}_j(\tau)}\right| = \left|\frac{row_i[A] \times column_j\,[e^{A\tau}]}{row_j[A] \times column_j\,[e^{A\tau}]}\right| \tag{3.6}$$

It can be observed in (3.6) that the calculated sensitivity is independent of the amount of perturbation of state z_j and is only a function of time. The sensitivity should be determined after a small amount of time, τ, that is selected based on the response speed of the system. In order to pick a suitable instant, eigenvalues of matrix A that represent the speed of convergence or divergence of the states of the system are considered. The eigenvalues with negative real parts correspond to the states that can be stabilized and therefore they are of no concern. On the other hand, in the set of all eigenvalues with positive real parts, the one that has the largest real part shows the fastest divergence and can be considered as a measure for the speed of the system. Consequently, the time instant τ is when the value of the state corresponding to the eigenvalue, which possesses the largest positive real part, changes by 0.1%.

Therefore, the calculated sensitivity can be utilized as a dependency measure of states to put all decoupled states in different partitions that are going to be controlled separately. The larger the sensitivity is, the more z_i is dependent to z_j. Note that in (3.6), all of the states are non-dimensionalized with respect to the equilibrium point.

3.2 Decoupling Criteria and Objective Function

The notion of sensitivity can be considered as a metric in the space of system states to represent the amount of coupling of every two states of the system. This is similar to the distance between data points in clustering algorithms. However, the larger the value of sensitivity is, the more coupled a state is with respect to another. In the clustering methods, an objective function is normally defined to find an optimum clustering result in the space of different possible clusterings based on the following two criteria: a) separation between the clusters, and b) compactness of the clusters. In each optimization iteration, a set of points is selected to be the cluster centers, and hence, the abovementioned criteria can be calculated with respect to them. The compactness of the clusters can be checked through the sum of distances between the data points in a cluster and the center. In addition, the separation between the clusters is formulated based on the distances between the centers of the clusters. It is worth mentioning that occasionally the number of clusters should be known before the clustering process.

In the case of partitioning of the states of a system, the aim is to find the most coupled sub-systems. In other words, the states with the largest value of sensitivity with respect to

each other must be placed in the same partition. Therefore, to define a suitable objective function for partitioning purposes, a criterion can be deemed based on the average amount of sensitivity in the partitions with respect to the chosen center states of the partitions. Furthermore, various systems may have different constraints in terms of placing certain states next to each other in the partitioning process. These constraints are taken into account by defining weight functions in averaging the sensitivity values of partitions. Consequently, a weighted average function is used to average the sensitivity values in the partitions as an objective function. This average is summed on all of the partitions and the resulting criterion is called *mean sensitivity*. Therefore, mean sensitivity can be calculated as:

$$M = \sqrt{\frac{1}{\sum_{i=1}^{m}\sum_{k=1}^{n_i} w_{ik}} \sum_{i=1}^{m}\sum_{k=1}^{n_i} w_{ik} S^2(z_k^i, z_c^i)} \tag{3.7}$$

where,

m = number of partitions,

n_i = number of states in the ith partition,

z_k^i= the kth state in the ith partition,

z_c^i = the center state in the ith partition,

w_{ik} = weight of z_{ik} belonging to the ith partition.

The weight function is selected in the range of 0 to 1. The higher the value of the weight function, the more probable the according state is to be placed in a partition. However, since the weight function shows a relative desire of including a state in a partition, if its value is constant for all of the states, it implies no priority in the partitioning process.

Another objective that should be considered in partitioning of a system is the dimension of the system. It is more desirable to have equal dimensions of the sub-systems. Therefore, another criterion, namely *uniformity*, is defined based on the distribution of the states of the system in the different partitions. The well-known statistical function, variance function, has been utilized for this purpose. In this criterion the deviation of each sub-system's dimension from the average number of the states in the partitions is calculated and averaged based on the mean square average function. Generally speaking, this criterion checks the distribution of the states in different partitions.

Therefore, the uniformity is the variance of the number of elements in the partitions with respect to the average number of elements that can be defined as:

$$U = \sqrt{\frac{1}{m}\sum_{i=1}^{m}(n_i - \frac{n}{m})^2} \tag{3.8}$$

Based on the above definitions, in order to obtain the optimum partitioning of a system the mean sensitivity should be maximized while the uniformity is minimized. To simplify the optimization process, a linear combination of the criteria can be used to define one objective function that incorporates both aspects. In this way, the dimensions of these criteria are unified [24]. This function is defined as:

$$J = \frac{1}{n}U - M \tag{3.9}$$

where *n* is the total number of states and the factor $\frac{1}{n}$ normalizes the uniformity.

Since the uniformity and mean sensitivity are considered with plus and minus sign, respectively, minimizing *J*, would result in minimizing and maximizing the uniformity and mean sensitivity, sequentially.

3.3 Decoupling Algorithm

In this section, a step-by-step algorithm for the decoupling method discussed above is given. This algorithm consists of two optimization loops. For a given set of centers of the partitions, the inner optimization is performed to place the states in the suitable partitions. However, since there exists a number of different choices to pick the center states, an outer loop optimization with respect to an objective function is done to select the best partitioning. The algorithm can be detailed as follows:

1. In this partitioning method, the number of partitions should be known in *a priori*. Therefore, before starting the partitioning process, the number of partitions or sub-systems should be chosen.
2. At each outer loop iteration, a system state is placed in the empty partitions as the center of the partition with respect to which sensitivity analysis is performed.
3. The sensitivity of each of the remaining states with respect to the center states is calculated.
4. In the inner loop optimization, the maximum sensitivity of each state with respect to the center states is selected and the state is transferred to the corresponding partition.

5. In this way, if the number of partitions is shown by m and the number of states by n, then $\binom{n}{m}$ different partitionings can be constructed out of which the one that optimizes the associated objective function should be picked. Hence, in this step the objective function for each possible partitioning is calculated.
6. The best partitioning is identified as the one that minimizes the objective function.

Determining the number of partitions depends entirely on the type of system. In order to be adaptable and flexible for different systems, choosing this amount has been made so that it can be applicable to most systems. Every system has its own objectives and constraints and by using these criteria, a suitable amount of partitions can be chosen.

3.4 Sub-systems Construction

Subsequently, the LTI system should be divided into a number of reduced-dimension linear sub-systems based on the partitions in the previous section. These sub-systems can be identified by a set of matrices, $\{(A_i, B_i, C_i)|i = 1, \dots, m\}$. The A_i matrix is evaluated by considering only the rows and columns of A that correspond to the states that appear in the i^{th} partition. In order to construct B_i, first the input states in partition i are identified. The rows of B that correspond to all of the states in the i^{th} partition and columns of B for the input states are selected and the rest of the elements are neglected. For C_i, the output states in the partition i are found. The rows of C corresponding to the output states in the i^{th} partition and the columns of C for all existing states in partition i are kept and the rest of the elements of C are neglected to construct C_i.

4 Chapter 4: Simulation and Results

In this chapter, the abovementioned decoupling algorithm is utilized to divide a large 540 MWe PHWR into three sub-systems. An optimal controller is designed for the system. Based on the achieved sub-systems, the centralized controller is split to three sub-controllers that separately control the sub-systems.

4.1 Partitioning of a Large 540 MWe PHWR

The system was modeled and simulated using MATLAB®. The sensitivity was taken at τ = 0.1 seconds. Three partitions were chosen and the simulation yielded the first partition having 20 states, the second having 27 states and the third having 25 states. The partitions are given in Table 4.1,

Zone	Partition 1	Partition 2	Partition 3
1	z_1, z_{15}, z_{29}, z_{43}, z_{57}		
2	z_2, z_{16}, z_{30}, z_{44}, z_{58}		
3		z_3, z_{17}, z_{31}, z_{45}, z_{59}	
4		z_4, z_{18}, z_{32}, z_{46}, z_{60}	
5		z_5, z_{19}, z_{33}, z_{47}, z_{61}	
6		z_6, z_{20}, z_{34}, z_{48}, z_{62}	
7		z_7, z_{21}, z_{35}, z_{49}, z_{63}	
8	z_8, z_{22}, z_{36}, z_{50}, z_{64}		

9	$z_9, z_{23}, z_{37}, z_{51}, z_{65}$		
10			$z_{10}, z_{24}, z_{38}, z_{52}, z_{66}$
11			$z_{11}, z_{25}, z_{39}, z_{53}, z_{67}$
12			$z_{12}, z_{26}, z_{40}, z_{54}, z_{68}$
13			$z_{13}, z_{27}, z_{41}, z_{55}, z_{69}$
14			$z_{14}, z_{28}, z_{42}, z_{56}, z_{70}$
		z_{71}, z_{72}	

Table 4.1: Simulation results of partitions

where states 1-14 are the corresponding zonal iodine concentrations, 15-28 the xenon concentrations, 29-42 the delayed neutron concentrations, 43-56 the water levels, 57-70 the powers, 71 the fuel temperature, and 72 the coolant temperature. The center of each partition that was randomly chosen was state 15, xenon concentration in zone 1, for partition 1, state 20, xenon concentration in zone 6, for partition 2, and state 27, xenon concentration for zone 13. It is completely reasonable that the center states of the partitions were the xenon concentrations since this system's purpose revolves around controlling this.

The corresponding zonal water levels were logically placed in the partition that had the most states for its zone since they depend only on the input to the system and would yield zeros for sensitivity thus being grouped together.

From the partition results, it can be seen that the states were divided into the three partitions according to which states they were most coupled with. These states correspond to the most coupled zones which were defined through the coupling coefficients. The coupling coefficients between non-neighbouring zones and its own zone are assumed to be zero. For neighbouring zones, the coupling coefficients were calculated based on the area of interface and the distance between the *i*th and *j*th zones. Through these relationships, the model was decoupled. Therefore, an optimal distribution of states were acquired that can be used for controller design.

4.2 Centralized Controller

The whole system is modeled in MATLAB Simulink®. A MATLAB function, called *care*, is used to solve the Algebraic Ricatti Equation for the system and identify the corresponding control gain. The same function is employed to obtain an optimal full-state observer for the control system. In Appendix A, all the elements of the controller and observer matrices are listed. Both the controller and observer are placed in the centralized control loop of the modeled system. The Simulink model of the system with the centralized controller is shown in Fig. 4.1. The system is disturbed by changing the reactivity of zone 1. Different amounts of disturbance to the system limits, ±3.5 mk, are considered and the behaviour of the system is studied. The disturbance functions are shown in Fig. 4.2. The change in global power of the reactor as the system response for different disturbance functions is depicted in Fig. 4.3 and Fig. 4.4. The overall behaviour of the system is almost the same for various disturbance magnitudes. The overshoot of

the system increases proportional to the amount of disturbance. However, the response time is almost the same for all different disturbance functions. Fig. 4.5 shows an example of the response of the system to the +3.5 mk versus -3.5 mk disturbance functions. These figures illustrate that the system response is not symmetric with respect to the line Global Power = 1800 MW. The overshoot of the system response to all of the disturbance functions is plotted in Fig. 4.6 that shows an almost linear trend for both positive and negative disturbances. The values of overshoot are not symmetric with respect to the line Global Power = 1800 MW. The values of the second peak of the system response to different positive and negative disturbances can be observed in Fig. 4.7. They also show a linear behaviour with respect to different disturbance functions, however, they are not symmetric with respect to the line Global Power = 1800 MW.

Based on the response of the system, the maximum overshoot occurs for the disturbance of ±3.5 mk. For the positive maximum disturbance, the overshoot of the system is 79 MW and similarly for the negative maximum disturbance, the overshoot value is 80.5 MW. The response time of the system for all disturbances is almost the same around 200 seconds. The steady state error of the response is also constant for different disturbances and is -0.5 MW which is negligible for this system.

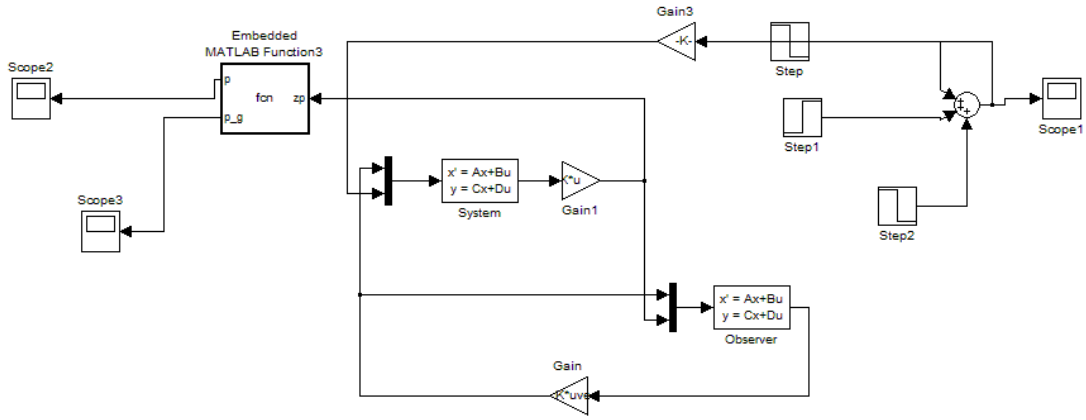

Figure 4.1: Centralized system

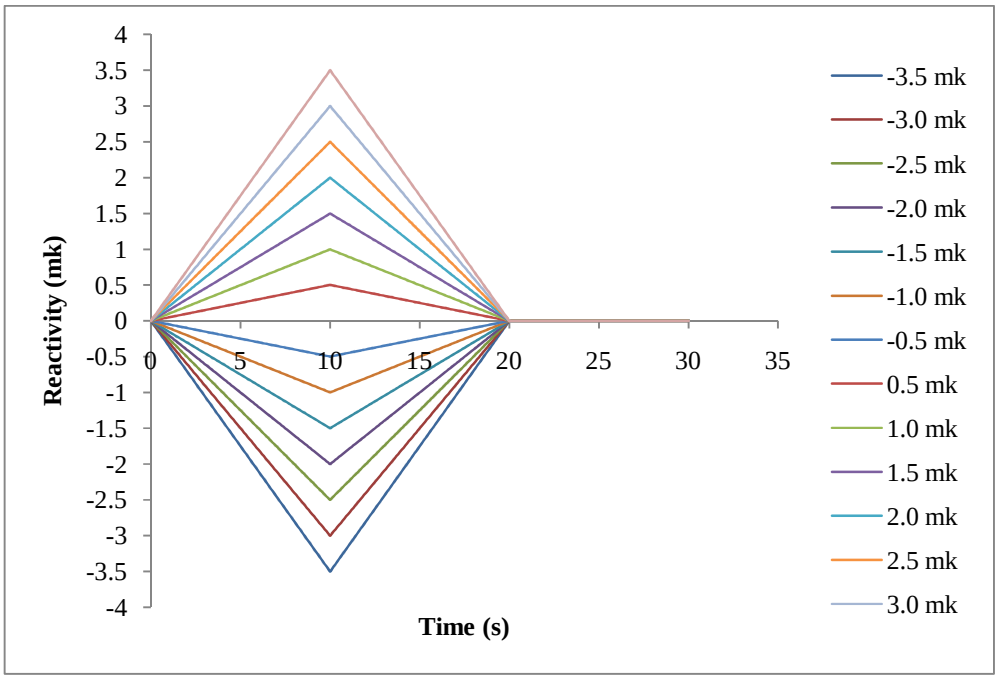

Figure 4.2: Disturbance functions

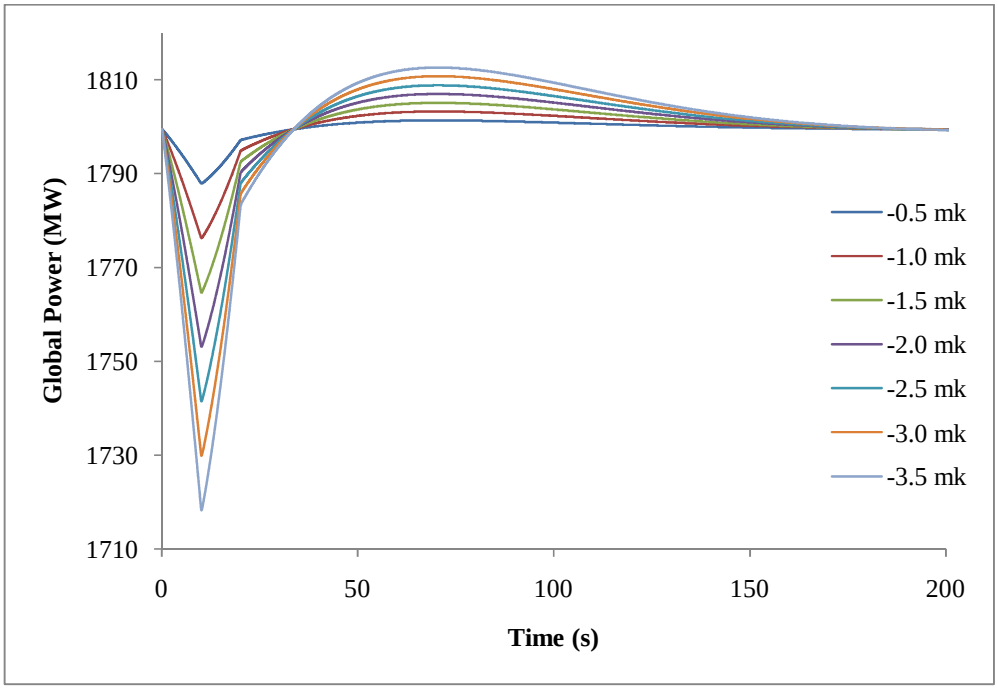

Figure 4.3: System response for negative reactivity disturbances of a centralized controller

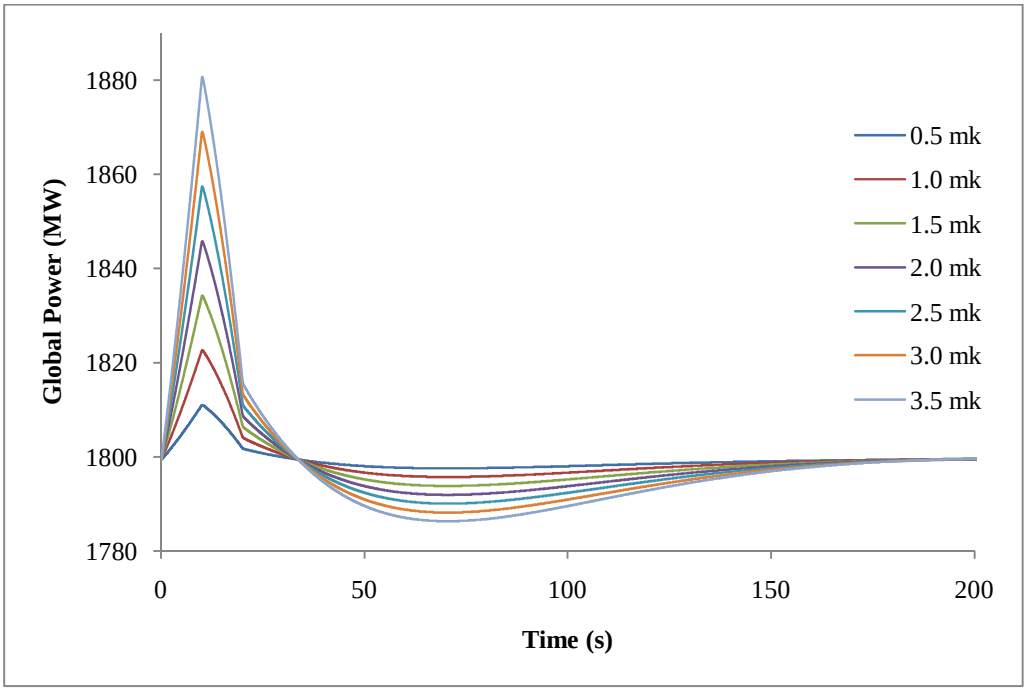

Figure 4.4: System response for positive reactivity disturbances of a centralized controller

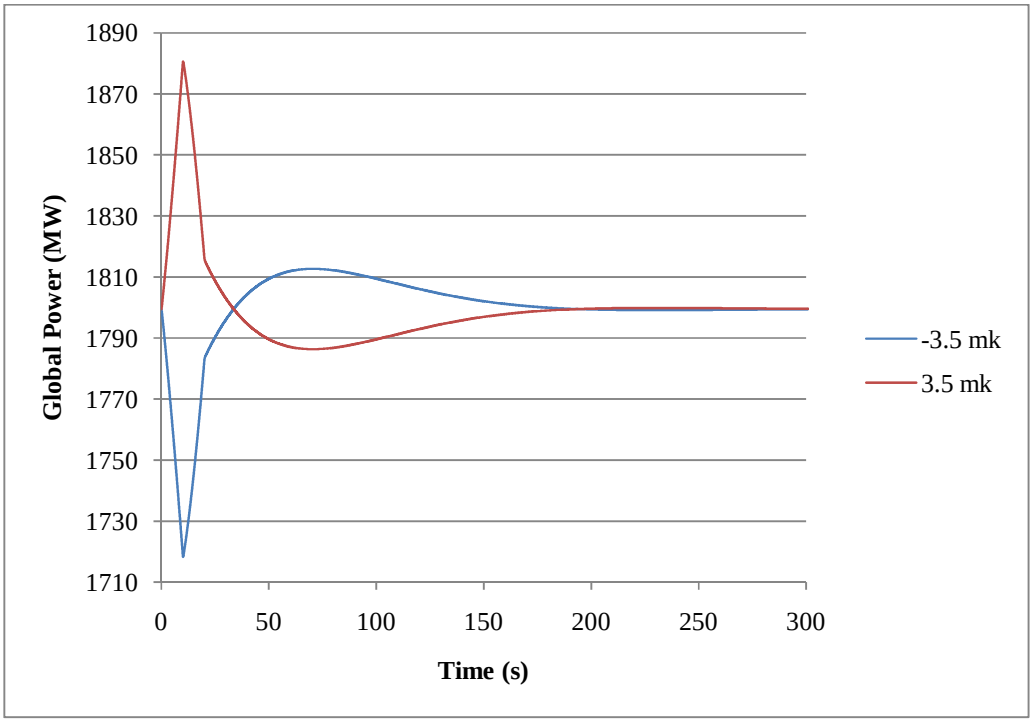

Figure 4.5: System response of ± 3.5 mk disturbance using a centralized controller

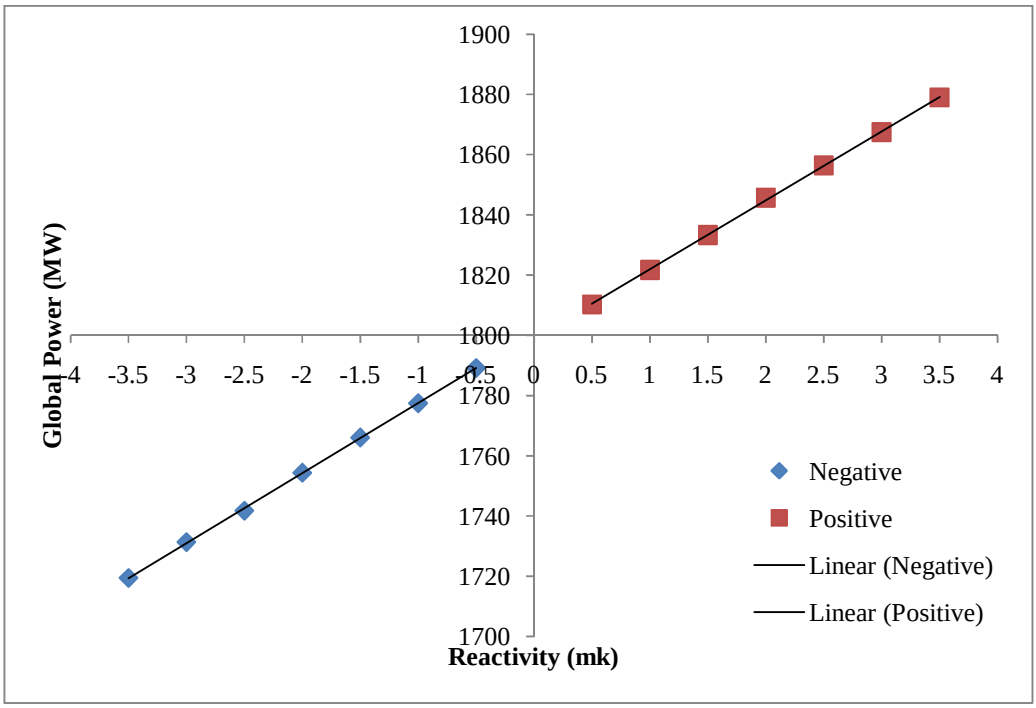

Figure 4.6: Overshoot of the system response for both positive and negative reactivity disturbances using a centralized controller

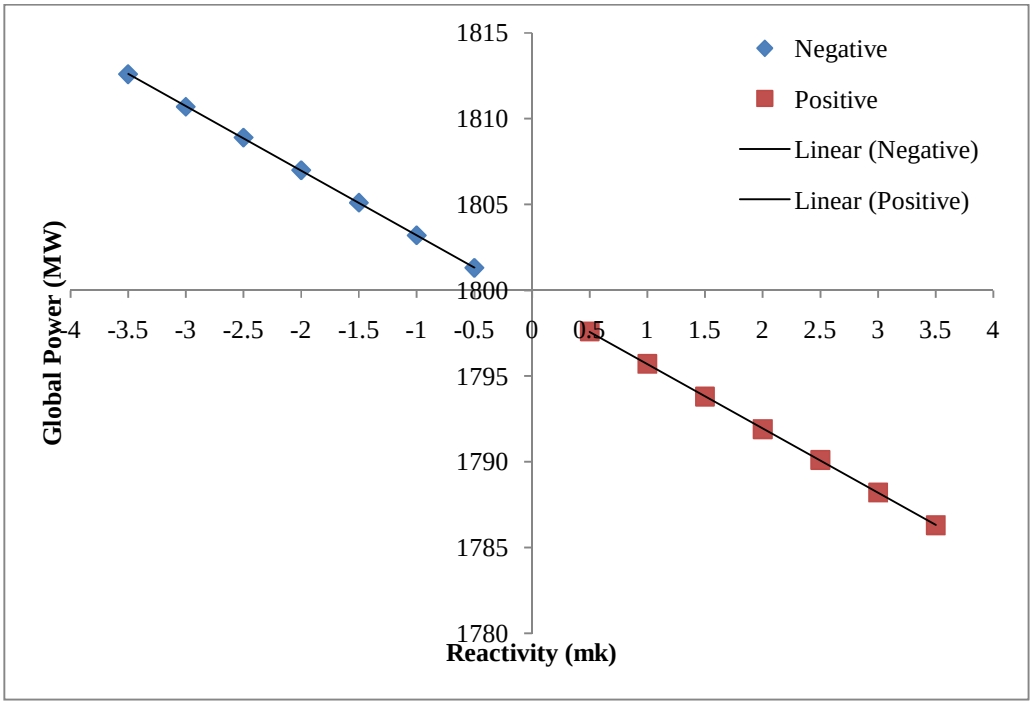

Figure 4.7 Second peak of the system response for both positive and negative reactivity disturbances using a centralized controller

4.3 Decentralized Controllers

In order to design decentralized controllers, the centralized controller should be broken down based on the system partitioning of the states of the system in Section 4.1. The 14×72 matrix of the control gains shown in Table A.1 is divided into three sub-controllers considering the control gains corresponding to the existing states in each partition of the states. The rows of the sub-controller matrices correspond to the input variables to the system that should be determined and the number of them is 14 for all sub-controllers. Therefore, if a partition does not include an input variable, then the relevant row is equal to zero. Each column of a sub-controller is associated to a state of the system in a partition. Hence, the number of columns is equal to the number of states

in a partition and the corresponding gain is picked from the centralized controller for all states in different sub-controllers. Finally, the designed decentralized controller for a large PHWR can be shown by three gain matrices: $K_1(14 \times 20)$, $K_2(14 \times 27)$, and $K_3(14 \times 25)$. Each sub-controller is working with the corresponding sub-system. The calculated input variables from all sub-controllers are summed to determine the final input to the system. Note that the sub-controllers do not contribute to the input variables that do not exist in the corresponding partitions.

The Simulink model of the system with the decentralized controllers is shown in Fig. 4.8. The same observer and disturbance functions are utilized for the decentralized system. The system partitioning is performed after calculating the estimated values for the system states. The change in global power of the reactor as the system response for different disturbance functions is depicted in Fig. 4.9 and Fig. 4.10. The overall behaviour of the system is almost the same for various disturbance magnitudes. The overshoot of the system increases proportional to the amount of disturbance. However, the response time is almost the same for all different disturbance functions. Fig. 4.11 shows an example of the response of the system to the +3.5 mk versus -3.5 mk disturbance functions. These figures illustrate that the system response is not symmetric with respect to the line Global Power = 1800 MW. The overshoot of the system response to all of the disturbance functions is plotted in Fig. 4.12 that shows an almost linear trend for both positive and negative disturbances. The values of overshoot are not symmetric with respect to the line Global Power = 1800 MW. The values of the second peak of the system response to different positive and negative disturbances can be observed in Fig. 4.13. They also show

a linear behavior with respect to different disturbance functions, however, they are not symmetric with respect to the line Global Power = 1800 MW.

Based on the response of the system, the maximum overshoot occurs for the disturbance of ±3.5 mk. For the positive maximum disturbance, the overshoot of the system is 87 MW and similarly for the negative maximum disturbance, the overshoot value is 87.6 MW. The response time of the system for all disturbances is almost the same and around 500 seconds. The steady state error of the response is also constant for different disturbances and is -0.6 MW which is negligible for this system.

In Fig. 4.14, the response of the system to ±3.5 mk disturbance is shown for both the centralized and decentralized controllers. Since the coupling between the states of the system in different sub-systems is neglected in the design of the decentralized controller, using this type of controller makes the system slower with a larger overshoot. However, in terms of implementation of the controller in the real world, any sub-controller can be mounted at the corresponding sub-system which would reduce the wiring and maintenance required. Since the zones in a large reactor are coupled, any change in control input to any zone would cause a respective change in the neutron flux to the neighboring zones, which may not desirable in the control of reactor. In the case of the decentralized controllers, the most coupled states of the system are controlled together, which would help make it easier to achieve a uniform power distribution across the reactor core.

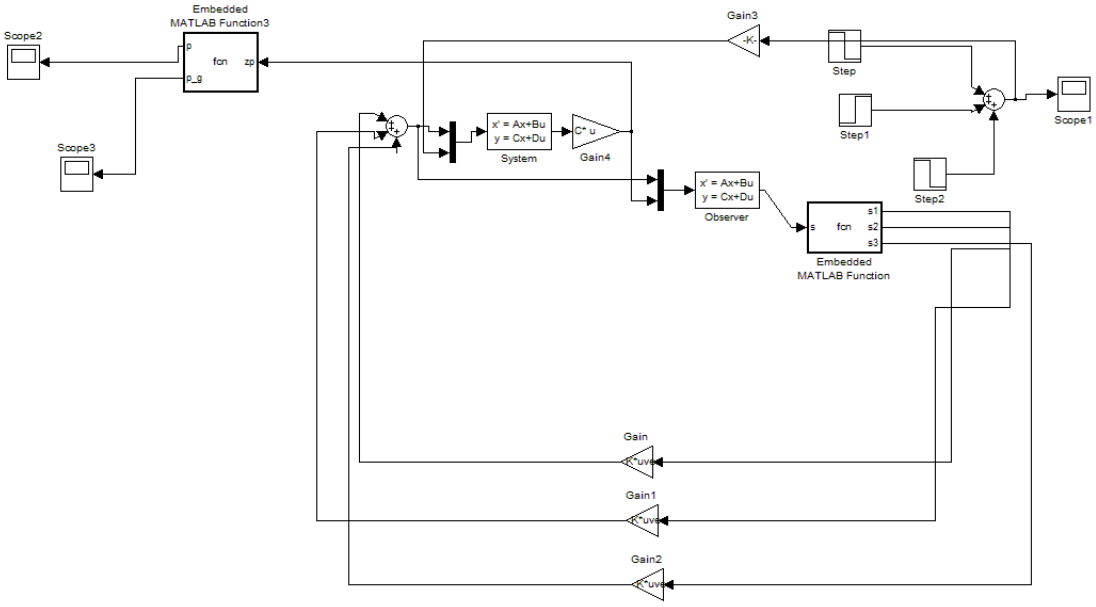

Figure 4.8: Decentralized system

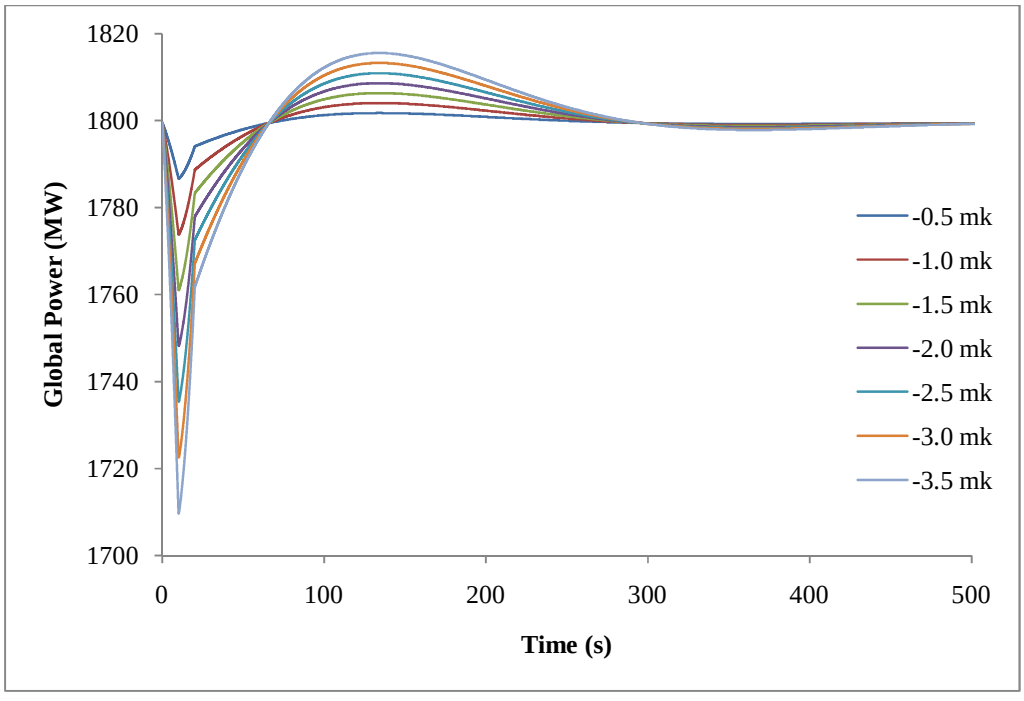

Figure 4.9: System response for negative reactivity disturbances of decentralized controllers

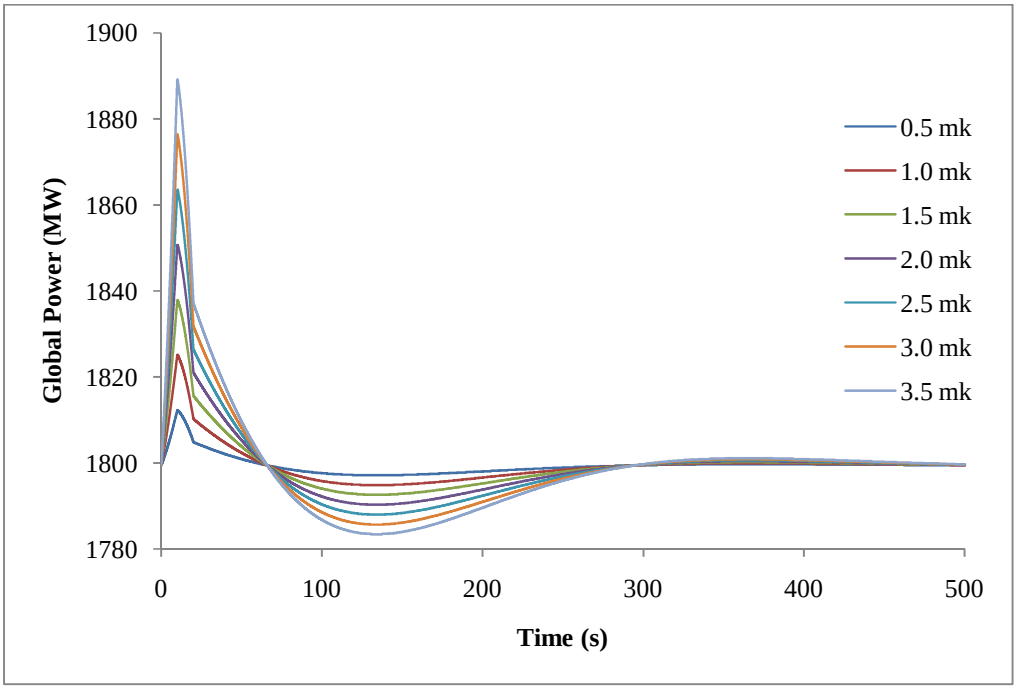

Figure 4.10: System response for positive reactivity disturbances of decentralized controllers

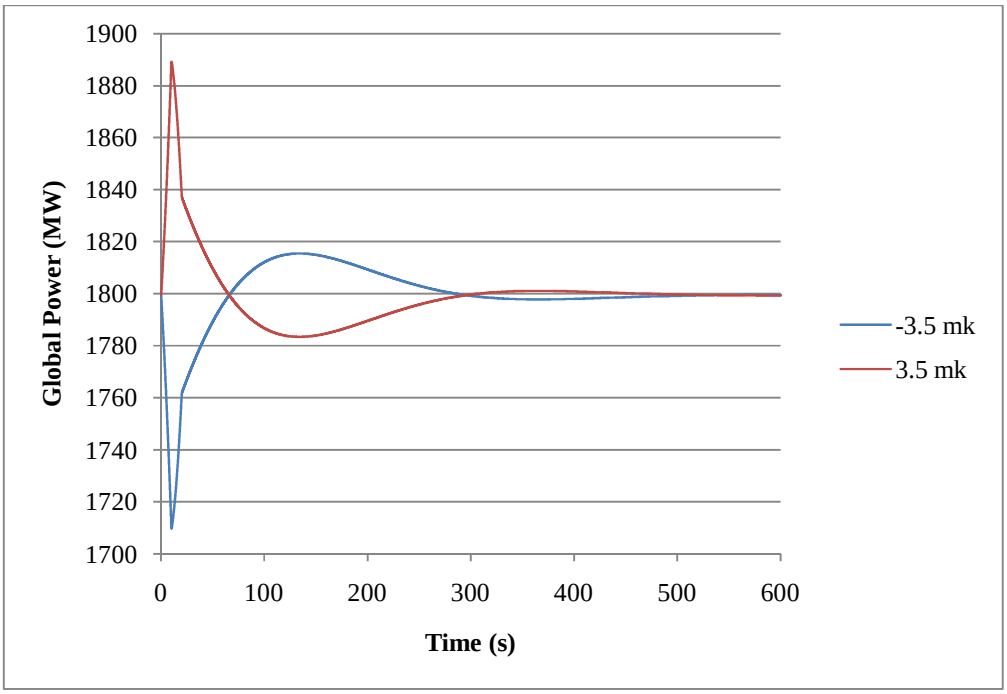

Figure 4.11: System response of ± 3.5 mk disturbance using decentralized controllers

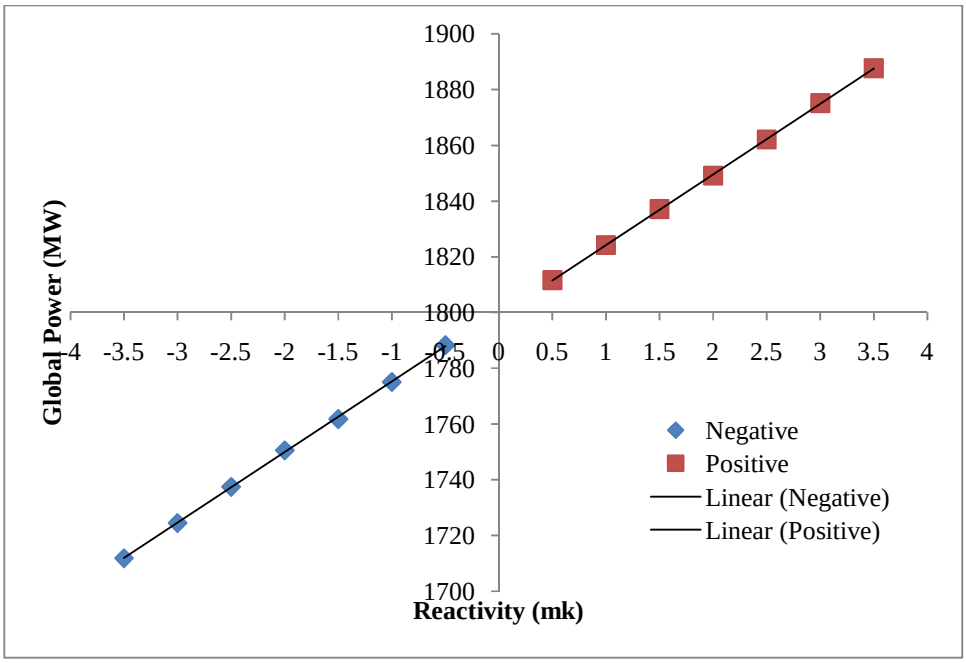

Figure 4.12: Overshoot of the system response for both positive and negative reactivity disturbances using decentralized controllers

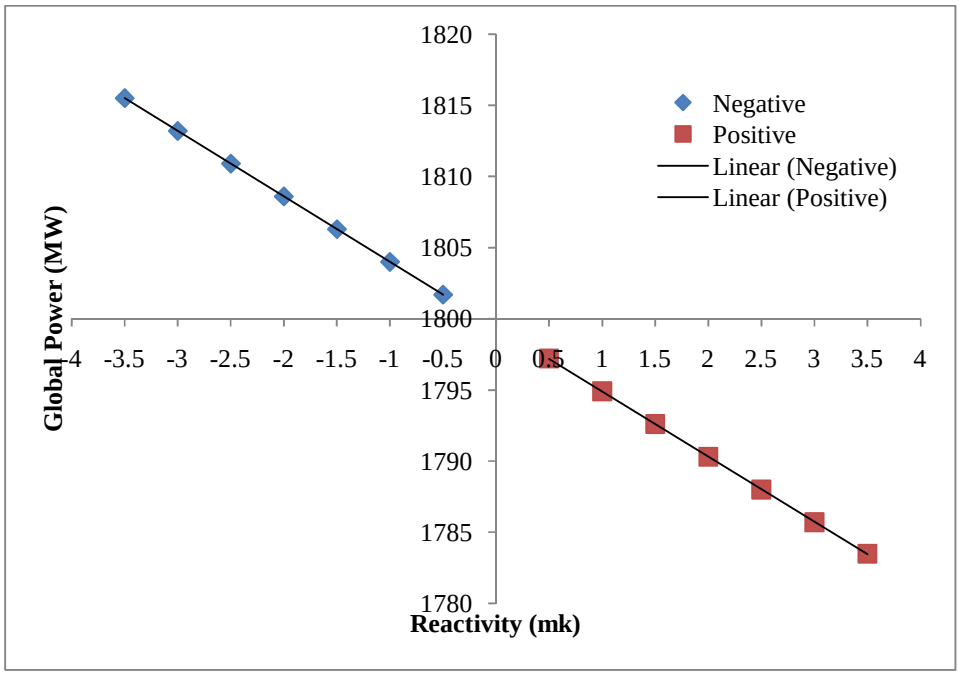

Figure 4.13: Second peak of the system response for both positive and negative reactivity disturbances using decentralized controllers

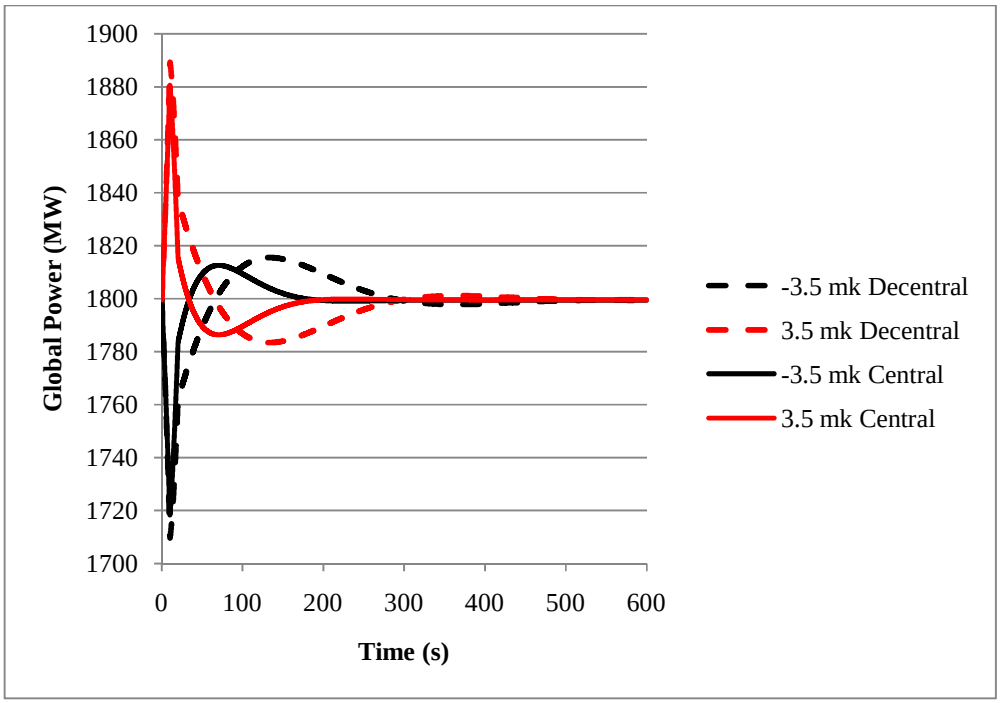

Figure 4.14: System response to ±3.5 mk disturbance for both the centralized and decentralized controllers

4.4 Fail-Safe Study of Decentralized Versus Centralized Controllers

Fail-safe study of a system attempts to simulate the worst case scenarios that can happen to the system and investigate whether the system can survive. This study is valuable especially when the result of any failure in the system can be disastrous. In this thesis, a centralized controller has been divided into several decentralized controllers located at different sections of a reactor. This will reduce the risk of losing all the control signals at once.

In this section, a worst case scenario is simulated for the system under study in this thesis considering both centralized and decentralized controllers. The simulation is done in MATLAB Simulink® and the results are shown in Fig. 4.15 and Fig. 4.16.

Consider a scenario that a large PHWR is compensating for a disturbance of ±3.5 mk and suddenly the centralized controller stops working after 200 seconds for a few minutes. As the result, it can be observed in Fig. 4.15, for the maximum positive reactivity, +3.5 mk, the global power reaches to 2150 MW in about 10 minutes as the system is being rectified. At this point, the reactor core would go into meltdown. However, as shown in Fig. 4.16, in the case of employing decentralized controllers for the maximum positive reactivity, +3.5 mk, if one of the controllers shuts down for 10 minutes, the global power reaches to 1815 MW that is in the safe range.

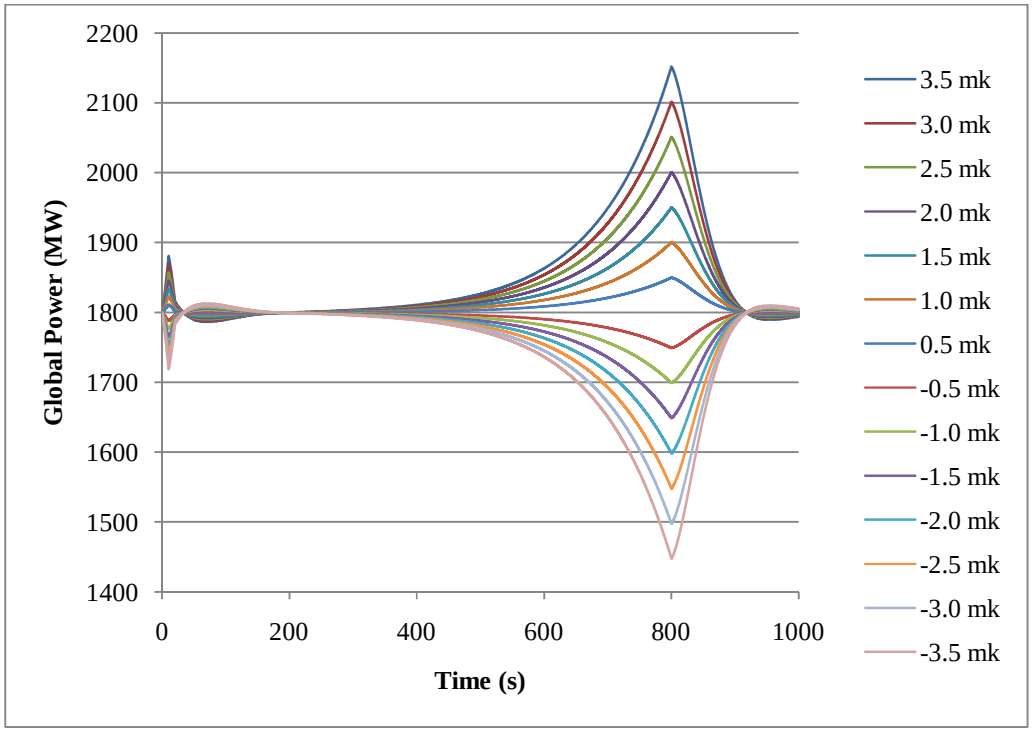

Figure 4.15: Fail-safe response of a centralized controller

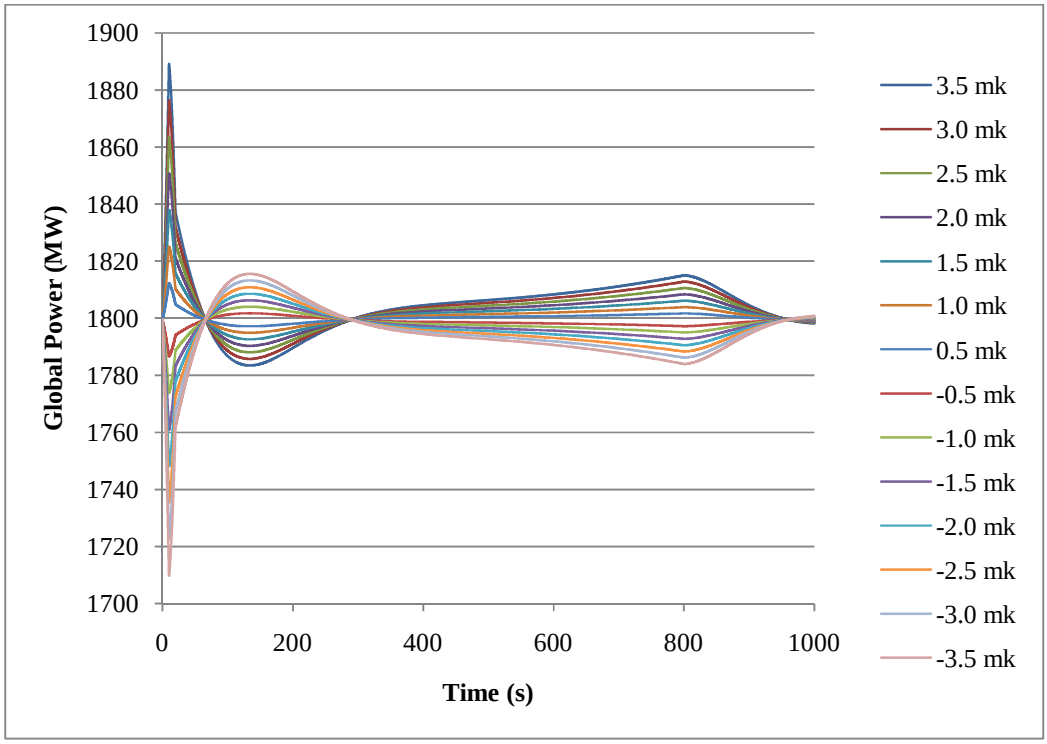

Figure 4.16: Fail-safe response of decentralized controllers

In the case of the centralized controller, if the controller shuts down for a few minutes, since the system does not receive any control signals, it goes unstable, rapidly, and hits the safety margins of the system. On the other hand, when a centralized controller is substituted with a number of decentralized controllers, any failure of a controller can be compensated by other controllers for a much longer time. Therefore, one of the advantages of decentralized controllers is that they are more fail-safe than a centralized controller.

5 Chapter 5: Conclusion and Future Work

This thesis has designed and implemented optimal decentralized controllers using the reactor nodal model of a large 540 MWe PHWR to control the xenon induced spatial oscillations. A decoupling algorithm was developed and tested using this model to create a decentralized system of controllers. A centralized controller was designed to compare both approaches.

In this thesis, it can be seen that the decentralized controllers have a similar system response to the centralized controller after a reactivity disturbance to the system's limits of ±3.5 mk in the first zone. The most significant difference was in the response time where the decentralized system was around 500 seconds while the centralized system was around 200 seconds. For both controllers, the overshoot of the system response to all of the disturbance functions showed an almost linear trend for both the positive and negative disturbances. The decentralized controllers had slightly larger overshoots of around 10 MW than the centralized controllers. The steady-state errors were relatively close, -0.5 MW for the centralized and -0.6 MW for the decentralized systems. Overall, the centralized controller showed a faster and better performance. Given that the coupling between the states of the system in the different sub-systems is neglected in the design of the decentralized controllers, this could be expected. However, the advantages that a decentralized system has over a centralized system should be considered such as the ability to fail-safe. This example was given proving that the decentralized controllers are more fail-safe than the centralized. In addition to this, less wiring, lower maintenance, and lower costs are also advantages. With this research work, these advantages can be

further explored in future work. A communication network of a Distributed Control System (DCS) can be implemented so that the decentralized controllers can communicate with each other by networks. In this way, the information of the states of the system will not be lost and can be accessed and shared throughout the network. This could potentially improve the system's performance in addition to acquiring the advantages proposed by modern control technologies.

Appendices

Appendix A: Controller and Observer Gains

$K = \left[K_I{}^T \ K_X{}^T \ K_C{}^T \ K_H{}^T \ K_P{}^T \ K_{T_f} K_{T_c} \right]^T$														
K_I	0.090	0.002	0.002	0.001	0.000	0.000	0.000	0.001	0.000	0.000	0.000	0.000	0.000	0.000
	0.002	0.092	0.000	0.001	0.002	0.000	0.000	0.000	0.001	0.000	0.000	0.000	0.000	0.000
	0.002	0.000	0.068	0.002	0.000	0.002	0.000	0.000	0.000	0.001	0.000	0.000	0.000	0.000
	0.000	0.000	0.001	0.097	0.001	0.000	0.000	0.000	0.000	0.000	0.001	0.000	0.000	0.000
	0.000	0.003	0.000	0.002	0.078	0.000	0.003	0.000	0.000	0.000	0.000	0.001	0.000	0.000
	0.000	0.000	0.002	0.001	0.000	0.090	0.002	0.000	0.000	0.000	0.000	0.000	0.001	0.000
	0.000	0.000	0.000	0.001	0.002	0.002	0.092	0.000	0.000	0.000	0.000	0.000	0.000	0.001
	0.001	0.000	0.000	0.000	0.000	0.000	0.000	0.090	0.002	0.002	0.001	0.000	0.000	0.000
	0.000	0.001	0.000	0.000	0.000	0.000	0.000	0.002	0.092	0.000	0.001	0.002	0.000	0.000
	0.000	0.000	0.001	0.000	0.000	0.000	0.000	0.002	0.000	0.068	0.002	0.000	0.002	0.000
	0.000	0.000	0.000	0.001	0.000	0.000	0.000	0.000	0.000	0.001	0.097	0.001	0.000	0.000
	0.000	0.000	0.000	0.000	0.001	0.000	0.000	0.000	0.003	0.000	0.002	0.078	0.000	0.003
	0.000	0.000	0.000	0.000	0.000	0.001	0.000	0.000	0.000	0.002	0.001	0.000	0.090	0.002
	0.000	0.000	0.000	0.000	0.000	0.000	0.001	0.000	0.000	0.000	0.001	0.002	0.002	0.092
K_X	3.223	1.723	1.529	0.552	1.189	1.369	1.150	1.301	1.034	0.825	0.304	0.818	0.913	0.834
	1.720	3.234	0.980	0.560	1.857	1.148	1.424	1.033	1.340	0.666	0.312	1.051	0.833	0.966
	1.560	1.002	2.084	0.472	0.853	1.560	1.002	0.842	0.681	0.738	0.238	0.596	0.842	0.681
	0.546	0.554	0.457	0.687	0.554	0.546	0.554	0.300	0.308	0.229	0.127	0.289	0.300	0.308
	1.200	1.878	0.843	0.566	2.713	1.200	1.878	0.826	1.063	0.590	0.296	1.109	0.826	1.063
	1.369	1.150	1.529	0.552	1.189	3.223	1.723	0.913	0.834	0.825	0.304	0.818	1.301	1.034
	1.148	1.424	0.980	0.560	1.857	1.720	3.234	0.833	0.966	0.666	0.312	1.051	1.033	1.340
	1.301	1.034	0.825	0.304	0.818	0.913	0.834	3.223	1.723	1.529	0.552	1.189	1.369	1.150
	1.033	1.340	0.666	0.312	1.051	0.833	0.966	1.720	3.234	0.980	0.560	1.857	1.148	1.424
	0.842	0.681	0.738	0.238	0.596	0.842	0.681	1.560	1.002	2.084	0.472	0.853	1.560	1.002
	0.300	0.308	0.229	0.127	0.289	0.300	0.308	0.546	0.554	0.457	0.687	0.554	0.546	0.554
	0.826	1.063	0.590	0.296	1.109	0.826	1.063	1.200	1.878	0.843	0.566	2.713	1.200	1.878
	0.913	0.834	0.825	0.304	0.818	1.301	1.034	1.369	1.150	1.529	0.552	1.189	3.223	1.723
	0.833	0.966	0.666	0.312	1.051	1.033	1.340	1.148	1.424	0.980	0.560	1.857	1.720	3.234
K_C	-0.131	-0.112	-0.089	-0.034	-0.094	-0.101	-0.097	-0.095	-0.090	-0.068	-0.026	-0.079	-0.084	-0.083
	-0.111	-0.136	-0.076	-0.034	-0.112	-0.096	-0.107	-0.089	-0.100	-0.064	-0.027	-0.088	-0.082	-0.089
	-0.091	-0.079	-0.078	-0.027	-0.072	-0.091	-0.079	-0.070	-0.066	-0.055	-0.020	-0.060	-0.070	-0.066
	-0.037	-0.038	-0.029	-0.015	-0.036	-0.037	-0.038	-0.028	-0.029	-0.022	-0.009	-0.028	-0.028	-0.029
	-0.094	-0.113	-0.069	-0.033	-0.116	-0.094	-0.113	-0.078	-0.089	-0.058	-0.025	-0.085	-0.078	-0.089
	-0.101	-0.097	-0.089	-0.034	-0.094	-0.131	-0.112	-0.084	-0.083	-0.068	-0.026	-0.079	-0.095	-0.090
	-0.096	-0.107	-0.076	-0.034	-0.112	-0.111	-0.136	-0.082	-0.089	-0.064	-0.027	-0.088	-0.089	-0.100
	-0.095	-0.090	-0.068	-0.026	-0.079	-0.084	-0.083	-0.131	-0.112	-0.089	-0.034	-0.094	-0.101	-0.097
	-0.089	-0.100	-0.064	-0.027	-0.088	-0.082	-0.089	-0.111	-0.136	-0.076	-0.034	-0.112	-0.096	-0.107
	-0.070	-0.066	-0.055	-0.020	-0.060	-0.070	-0.066	-0.091	-0.079	-0.078	-0.027	-0.072	-0.091	-0.079
	-0.028	-0.029	-0.022	-0.009	-0.028	-0.028	-0.029	-0.037	-0.038	-0.029	-0.015	-0.036	-0.037	-0.038
	-0.078	-0.089	-0.058	-0.025	-0.085	-0.078	-0.089	-0.094	-0.113	-0.069	-0.033	-0.116	-0.094	-0.113
	-0.084	-0.083	-0.068	-0.026	-0.079	-0.095	-0.090	-0.101	-0.097	-0.089	-0.034	-0.094	-0.131	-0.112
	-0.082	-0.089	-0.064	-0.027	-0.088	-0.089	-0.100	-0.096	-0.107	-0.076	-0.034	-0.112	-0.111	-0.136
K_H	-0.005	-0.002	-0.002	-0.001	-0.002	-0.002	-0.002	-0.002	-0.001	-0.001	0.000	-0.001	-0.001	-0.001
	-0.002	-0.005	-0.001	-0.001	-0.003	-0.002	-0.002	-0.001	-0.002	-0.001	0.000	-0.002	-0.001	-0.001
	-0.002	-0.001	-0.003	-0.001	-0.001	-0.002	-0.001	-0.001	-0.001	-0.001	0.000	-0.001	-0.001	-0.001
	-0.001	-0.001	-0.001	-0.001	-0.001	-0.001	-0.001	0.000	0.000	0.000	0.000	0.000	0.000	0.000
	-0.002	-0.003	-0.001	-0.001	-0.004	-0.002	-0.003	-0.001	-0.002	-0.001	0.000	-0.002	-0.001	-0.002
	-0.002	-0.002	-0.002	-0.001	-0.002	-0.005	-0.002	-0.001	-0.001	-0.001	0.000	-0.001	-0.002	-0.001
	-0.002	-0.002	-0.001	-0.001	-0.003	-0.002	-0.005	-0.001	-0.001	-0.001	0.000	-0.002	-0.001	-0.002
	-0.002	-0.001	-0.001	0.000	-0.001	-0.001	-0.001	-0.005	-0.002	-0.002	-0.001	-0.002	-0.002	-0.002
	-0.001	-0.002	-0.001	0.000	-0.002	-0.001	-0.001	-0.002	-0.005	-0.001	-0.001	-0.003	-0.002	-0.002
	-0.001	-0.001	-0.001	0.000	-0.001	-0.001	-0.001	-0.002	-0.001	-0.003	-0.001	-0.001	-0.002	-0.001
	0.000	0.000	0.000	0.000	0.000	0.000	0.000	-0.001	-0.001	-0.001	-0.001	-0.001	-0.001	-0.001
	-0.001	-0.002	-0.001	0.000	-0.002	-0.001	-0.002	-0.002	-0.003	-0.001	-0.001	-0.004	-0.002	-0.003
	-0.001	-0.001	-0.001	0.000	-0.001	-0.002	-0.001	-0.002	-0.002	-0.002	-0.001	-0.002	-0.005	-0.002
	-0.001	-0.001	-0.001	0.000	-0.002	-0.001	-0.002	-0.002	-0.002	-0.001	-0.001	-0.003	-0.002	-0.005
K_P	-0.001	-0.001	-0.001	0.000	-0.001	-0.001	-0.001	-0.001	-0.001	-0.001	0.000	-0.001	-0.001	-0.001
	-0.001	-0.001	-0.001	0.000	-0.001	-0.001	-0.001	-0.001	-0.001	-0.001	0.000	-0.001	-0.001	-0.001
	-0.001	-0.001	-0.001	0.000	-0.001	-0.001	-0.001	-0.001	-0.001	-0.001	0.000	-0.001	-0.001	-0.001
	0.000	0.000	0.000	0.000	0.000	0.000	0.000	0.000	0.000	0.000	0.000	0.000	0.000	0.000
	-0.001	-0.001	-0.001	0.000	-0.001	-0.001	-0.001	-0.001	-0.001	-0.001	0.000	-0.001	-0.001	-0.001
	-0.001	-0.001	-0.001	0.000	-0.001	-0.001	-0.001	-0.001	-0.001	-0.001	0.000	-0.001	-0.001	-0.001

	-0.001	-0.001	-0.001	0.000	-0.001	-0.001	-0.001	-0.001	-0.001	-0.001	0.000	-0.001	-0.001	-0.001
	-0.001	-0.001	-0.001	0.000	-0.001	-0.001	-0.001	-0.001	-0.001	-0.001	0.000	-0.001	-0.001	-0.001
	-0.001	-0.001	-0.001	0.000	-0.001	-0.001	-0.001	-0.001	-0.001	-0.001	0.000	-0.001	-0.001	-0.001
	-0.001	-0.001	-0.001	0.000	-0.001	-0.001	-0.001	-0.001	-0.001	-0.001	0.000	-0.001	-0.001	-0.001
	0.000	0.000	0.000	0.000	0.000	0.000	0.000	0.000	0.000	0.000	0.000	0.000	0.000	0.000
	-0.001	-0.001	-0.001	0.000	-0.001	-0.001	-0.001	-0.001	-0.001	-0.001	0.000	-0.001	-0.001	-0.001
	-0.001	-0.001	-0.001	0.000	-0.001	-0.001	-0.001	-0.001	-0.001	-0.001	0.000	-0.001	-0.001	-0.001
	-0.001	-0.001	-0.001	0.000	-0.001	-0.001	-0.001	-0.001	-0.001	-0.001	0.000	-0.001	-0.001	-0.001
${K_{T_f}}^T$	0.000	0.000	0.000	0.000	0.000	0.000	0.000	0.000	0.000	0.000	0.000	0.000	0.000	0.000
${K_{T_c}}^T$	-0.008	-0.009	-0.006	-0.003	-0.008	-0.008	-0.009	-0.008	-0.009	-0.006	-0.003	-0.008	-0.008	-0.009

Table A.1: Controller gains

$L = \left[L_I \ L_X \ L_C \ L_H \ L_P \ {L_{T_f}}^T {L_{T_c}}^T \right]^T$														
	-0.892	-0.003	0.040	0.059	0.003	0.003	0.001	0.000	0.000	0.004	0.005	0.000	0.000	0.000
	0.008	-0.895	0.008	0.062	0.014	0.003	0.002	0.001	0.000	0.001	0.005	0.002	0.001	0.000
	-0.037	-0.004	-0.867	0.061	0.000	-0.037	-0.004	-0.004	-0.001	0.001	0.004	0.000	-0.004	-0.001
	-0.060	-0.063	-0.052	-0.899	-0.077	-0.060	-0.063	-0.005	-0.005	-0.003	0.002	-0.005	-0.005	-0.005
	0.002	-0.009	0.005	0.082	-0.880	0.002	-0.009	0.000	-0.001	0.001	0.006	0.001	0.000	-0.001
	0.003	0.001	0.040	0.059	0.003	-0.892	-0.003	0.000	0.000	0.004	0.005	0.000	0.000	0.000
${L_I}^T$	0.003	0.002	0.008	0.062	0.014	0.008	-0.895	0.001	0.000	0.001	0.005	0.002	0.001	0.000
	0.000	0.000	0.004	0.005	0.000	0.000	0.000	-0.892	-0.003	0.040	0.059	0.003	0.003	0.001
	0.001	0.000	0.001	0.005	0.002	0.001	0.000	0.008	-0.895	0.008	0.062	0.014	0.003	0.002
	-0.004	-0.001	0.001	0.004	0.000	-0.004	-0.001	-0.037	-0.004	-0.867	0.061	0.000	-0.037	-0.004
	-0.005	-0.005	-0.003	0.002	-0.005	-0.005	-0.005	-0.060	-0.063	-0.052	-0.899	-0.077	-0.060	-0.063
	0.000	-0.001	0.001	0.006	0.001	0.000	-0.001	0.002	-0.009	0.005	0.082	-0.880	0.002	-0.009
	0.000	0.000	0.004	0.005	0.000	0.000	0.000	0.003	0.001	0.040	0.059	0.003	-0.892	-0.003
	0.001	0.000	0.001	0.005	0.002	0.001	0.000	0.003	0.002	0.008	0.062	0.014	0.008	-0.895
	-0.996	-0.004	0.046	0.064	0.004	0.003	0.001	0.001	0.000	0.005	0.005	0.000	0.001	0.000
	0.008	-0.996	0.009	0.068	0.016	0.004	0.003	0.001	0.000	0.002	0.005	0.002	0.001	0.000
	-0.042	-0.005	-0.995	0.067	0.000	-0.042	-0.005	-0.004	-0.001	0.001	0.005	0.000	-0.004	-0.001
	-0.067	-0.070	-0.060	-0.984	-0.087	-0.067	-0.070	-0.005	-0.006	-0.004	0.002	-0.006	-0.005	-0.006
	0.002	-0.010	0.006	0.089	-0.995	0.002	-0.010	0.000	-0.001	0.001	0.007	0.001	0.000	-0.001
	0.003	0.001	0.046	0.064	0.004	-0.996	-0.004	0.001	0.000	0.005	0.005	0.000	0.001	0.000
${L_X}^T$	0.004	0.003	0.009	0.068	0.016	0.008	-0.996	0.001	0.000	0.002	0.005	0.002	0.001	0.000
	0.001	0.000	0.005	0.005	0.000	0.001	0.000	-0.996	-0.004	0.046	0.064	0.004	0.003	0.001
	0.001	0.000	0.002	0.005	0.002	0.001	0.000	0.008	-0.996	0.009	0.068	0.016	0.004	0.003
	-0.004	-0.001	0.001	0.005	0.000	-0.004	-0.001	-0.042	-0.005	-0.995	0.067	0.000	-0.042	-0.005
	-0.005	-0.006	-0.004	0.002	-0.006	-0.005	-0.006	-0.067	-0.070	-0.060	-0.984	-0.087	-0.067	-0.070
	0.000	-0.001	0.001	0.007	0.001	0.000	-0.001	0.002	-0.010	0.006	0.089	-0.995	0.002	-0.010
	0.001	0.000	0.005	0.005	0.000	0.001	0.000	0.003	0.001	0.046	0.064	0.004	-0.996	-0.004
	0.001	0.000	0.002	0.005	0.002	0.001	0.000	0.004	0.003	0.009	0.068	0.016	0.008	-0.996
	0.223	0.004	-0.001	-0.006	-0.001	-0.001	0.000	0.002	0.000	-0.001	-0.001	0.000	0.000	0.000
	0.002	0.222	-0.001	-0.006	0.003	-0.001	0.000	0.000	0.002	0.000	-0.001	0.000	0.000	0.000
	0.011	0.001	0.220	-0.005	0.000	0.011	0.001	0.001	0.000	0.002	-0.001	0.000	0.001	0.000
	0.012	0.012	0.012	0.203	0.016	0.012	0.012	0.001	0.001	0.001	0.001	0.001	0.001	0.001
	0.000	0.006	-0.001	-0.008	0.220	0.000	0.006	0.000	0.000	0.000	-0.001	0.002	0.000	0.000
	-0.001	0.000	-0.001	-0.006	-0.001	0.223	0.004	0.000	0.000	-0.001	-0.001	0.000	0.002	0.000
${L_C}^T$	-0.001	0.000	-0.001	-0.006	0.003	0.002	0.222	0.000	0.000	0.000	-0.001	0.000	0.000	0.002
	0.002	0.000	-0.001	-0.001	0.000	0.000	0.000	0.223	0.004	-0.001	-0.006	-0.001	-0.001	0.000
	0.000	0.002	0.000	-0.001	0.000	0.000	0.000	0.002	0.222	-0.001	-0.006	0.003	-0.001	0.000
	0.001	0.000	0.002	-0.001	0.000	0.001	0.000	0.011	0.001	0.220	-0.005	0.000	0.011	0.001
	0.001	0.001	0.001	0.001	0.001	0.001	0.001	0.012	0.012	0.012	0.203	0.016	0.012	0.012
	0.000	0.000	0.000	-0.001	0.002	0.000	0.000	0.000	0.006	-0.001	-0.008	0.220	0.000	0.006
	0.000	0.000	-0.001	-0.001	0.000	0.002	0.000	-0.001	0.000	-0.001	-0.006	-0.001	0.223	0.004
	0.000	0.000	0.000	-0.001	0.000	0.000	0.002	-0.001	0.000	-0.001	-0.006	0.003	0.002	0.222
	0.997	0.003	-0.045	-0.066	-0.004	-0.003	-0.001	-0.001	0.000	-0.004	-0.005	0.000	-0.001	-0.001
	-0.009	0.997	-0.009	-0.068	-0.016	-0.004	-0.003	-0.001	0.000	-0.002	-0.005	-0.002	-0.001	0.000
	0.042	0.005	0.996	-0.067	0.000	0.042	0.005	0.004	0.001	-0.001	-0.005	0.000	0.004	0.001
	0.066	0.070	0.060	0.985	0.088	0.067	0.070	0.005	0.006	0.004	-0.002	0.006	0.005	0.006
${L_H}^T$	-0.002	0.010	-0.006	-0.089	0.996	-0.002	0.010	0.000	0.001	-0.001	-0.006	-0.001	0.000	0.001
	-0.003	-0.001	-0.046	-0.065	-0.004	0.997	0.004	-0.001	0.000	-0.005	-0.005	0.000	-0.001	0.000
	-0.003	-0.003	-0.009	-0.068	-0.016	-0.008	0.998	-0.001	0.000	-0.002	-0.005	-0.002	-0.001	0.000
	-0.001	0.000	-0.005	-0.005	-0.001	-0.001	0.000	0.997	0.004	-0.046	-0.065	-0.004	-0.003	-0.001
	-0.002	0.000	-0.002	-0.005	-0.002	-0.001	0.000	-0.008	0.998	-0.009	-0.068	-0.016	-0.004	-0.003
	0.005	0.001	-0.001	-0.005	0.000	0.004	0.001	0.041	0.005	0.996	-0.067	0.000	0.042	0.005

	0.006	0.006	0.004	-0.002	0.006	0.005	0.006	0.067	0.070	0.060	0.985	0.088	0.067	0.070
	0.000	0.001	-0.001	-0.007	-0.001	0.000	0.001	-0.003	0.010	-0.006	-0.089	0.996	-0.002	0.010
	-0.001	0.000	-0.005	-0.005	-0.001	-0.001	0.000	-0.003	-0.001	-0.046	-0.065	-0.004	0.997	0.004
	-0.001	0.000	-0.001	-0.005	-0.002	-0.001	0.000	-0.004	-0.003	-0.009	-0.068	-0.016	-0.008	0.997
$L_P{}^T$	1.348	0.304	0.390	0.254	0.117	0.130	0.071	0.197	0.083	0.100	0.072	0.044	0.048	0.031
	0.304	1.337	0.119	0.263	0.399	0.071	0.142	0.083	0.195	0.044	0.075	0.103	0.031	0.052
	0.390	0.119	1.111	0.267	0.086	0.390	0.119	0.100	0.044	0.155	0.072	0.036	0.100	0.044
	0.254	0.263	0.267	0.749	0.292	0.254	0.263	0.072	0.075	0.072	0.096	0.078	0.072	0.075
	0.117	0.399	0.086	0.292	1.181	0.117	0.399	0.044	0.103	0.036	0.078	0.168	0.044	0.103
	0.130	0.071	0.390	0.254	0.117	1.348	0.304	0.048	0.031	0.100	0.072	0.044	0.197	0.083
	0.071	0.142	0.119	0.263	0.399	0.304	1.337	0.031	0.052	0.044	0.075	0.103	0.083	0.195
	0.197	0.083	0.100	0.072	0.044	0.048	0.031	1.348	0.304	0.390	0.254	0.117	0.130	0.071
	0.083	0.195	0.044	0.075	0.103	0.031	0.052	0.304	1.337	0.119	0.263	0.399	0.071	0.142
	0.100	0.044	0.155	0.072	0.036	0.100	0.044	0.390	0.119	1.111	0.267	0.086	0.390	0.119
	0.072	0.075	0.072	0.096	0.078	0.072	0.075	0.254	0.263	0.267	0.749	0.292	0.254	0.263
	0.044	0.103	0.036	0.078	0.168	0.044	0.103	0.117	0.399	0.086	0.292	1.181	0.117	0.399
	0.048	0.031	0.100	0.072	0.044	0.197	0.083	0.130	0.071	0.390	0.254	0.117	1.348	0.304
	0.031	0.052	0.044	0.075	0.103	0.083	0.195	0.071	0.142	0.119	0.263	0.399	0.304	1.337
L_{T_f}	0.001	0.001	0.001	0.001	0.001	0.001	0.001	0.001	0.001	0.001	0.001	0.001	0.001	0.001
L_{T_c}	0.001	0.001	0.001	0.001	0.001	0.001	0.001	0.001	0.001	0.001	0.001	0.001	0.001	0.001

Table A.2: Observer gains

Appendix B: MATLAB Code of the Model

```
% Physical constants
l=7.9E-4;
lambda=9.1E-2;
Sigma_f=1.262E-3;
sigma_x=1.2E-18;
v=3.19E5;
gamma_I=6.18E-2;
lambda_x=2.1E-5;
beta=7.5E-3;
Sigma_a=3.2341E-3;
E_eff=3.2E-17;
gamma_x=6E-3;
D=0.9328;
lambda_I=2.878E-5;
m_d=1;
m_i=2;
K_i=-3.5E-5;
h_i0=100;
T_f0=547.2831;
T_c0=541.4037;
T_1=539;
mu_f=-3.4722E-6;
mu_c=3.33333E-5;
k_a=1.38428E-3;
k_b=4.238E-1;
k_c=1.758E-2;
k_d=4.3016759E-2;

% Zonal volumes
V=[14.723280,14.72328,17.633616,8.833968,17.633616,14.72328,14.723280,14.723280
,14.72328,17.633616,8.833968,17.633616,14.72328,14.723280]'.* 1.0e+06;

% Xenon absorption microscopic cross section
for i = 1:14
   sigmabar_x(i,1) = sigma_x/(E_eff*Sigma_f*V(i,1));
end

% Coupling coefficients
alpha = [0  5.607 8.4105 2.803  0  0   0    3.390  0  0  0  0  0  0
         5.607 0  0  2.803 8.4105  0   0    0  3.390  0  0  0  0  0
         9.650 0  0  4.824   0  9.650  0    0     0   3.39  0  0  0     0
         5.180 5.180 7.772   0  7.772  5.18 5.18  0   0  0  3.39  0  0  0
         0  9.650 0  4.824   0  0   9.65    0     0   0  0  3.390 0     0
         0  0  8.4105 2.803  0  0   5.607   0     0   0  0  0   3.39    0
         0  0  0  2.803 8.4105 5.607    0   0     0   0  0  0   0   3.39
```

```
    3.390 0  0  0    0    0    0   0   5.607 8.4105 2.803  0   0   0
    0  3.390 0  0    0    0    0   5.607  0  0  2.803 8.4105  0   0
    0  0  3.390 0    0    0    0   9.65   0  0  4.824    0 9.65  0
    0  0  0  3.39    0   0   0  5.180  5.180 7.772 0 7.772 5.18  5.18
    0  0  0  0  3.39 0    0    0   9.65   0    4.824  0   0  9.650
    0  0  0  0  0    3.39 0    0   0   8.4105  2.803  0   0  5.607
    0  0  0  0  0    0    3.39 0   0   0 2.803 8.4105 5.607    0]*l ;

% Steady state values
p0 =[132.75, 135.99, 123.30, 98.55, 140.40, 132.75, 135.99 132.75, 135.99, 123.30,
98.55, 140.40, 132.75, 135.99]';

I0 = (gamma_I*Sigma_f/lambda_I).*p0;

for i=1:14
   X0(i,1) =
((gamma_I+gamma_x)*Sigma_f*p0(i,1)/(lambda_x+sigmabar_x(i,1)*p0(i,1)));
end

C0 = (beta/(l*lambda)).*p0;

% A matrix
A=zeros(72,72);
for i = 1:14
   for j = 1:14
      P0(i,j) = p0(j,1)/p0(i,1);
   end
end
for i = 1:14
   for j=1:14
      if i==j
         A(56+i, 56+i) = (-1/l)*(beta+sum((alpha(i,:).*P0(i,:))')) + (1/l)*alpha(i,i)*P0(i,i);
      else
         A(56+i, 56+j) = (1/l)*alpha(i,j)*P0(i,j);
      end
   end
   A(56+i, 28+i) = (beta/l);
   A(56+i, 14+i) = -(sigmabar_x(i,1)*X0(i,1))/(l*Sigma_a);
   A(56+i, 42+i) = -K_i/l;
   A(56+i, 71) = mu_f/l;
   A(56+i, 72) = mu_c/l;
   A(28+i, 56+i) = lambda;
   A(28+i, 28+i) = -lambda;
   A(i, 56+i) = lambda_I;
   A(i,i) = -lambda_I;
   A(14+i, 56+i)= lambda_x - lambda_I * I0(i,1)/X0(i,1);
```

```
    A(14+i,i) = lambda_I * I0(i,1)/X0(i,1);
    A(14+i, 14+i) = -(lambda_x + sigmabar_x(i,1)*p0(i,1));
    A(71, 56+i) = k_a*P0(i,1);
end
A(71,71) = -k_b;
A(71,72) = k_b;
A(72,71) = k_c;
A(72,72) = -(k_c+k_d);

% B matrix
B=[zeros(42,14);-m_i*eye(14,14);zeros(16,14)];

% C matrix
C=[zeros(14,14) zeros(14,14) zeros(14,14) zeros(14,14) eye(14,14) zeros(14,1)
zeros(14,1)];

% Sensitivity matrix
tau=0.1;
eAt=expm(A.*tau);
S=A*eAt;

% Decoupling algorithm
J0=1e10;
for i0 = 1:72
    for j0 = i0+1:72
        for k0 = j0+1:72
            if (i0<=42 && i0>=57)
                Set1=[i0 14*3+mod(i0,14)];
            else
                Set1=[i0];
            end
            if (j0<=42 && j0>=57)
                Set2=[j0 14*3+mod(j0,14)];
            else
                Set2=[j0];
            end
            if (k0<=42 && k0>=57)
                Set3=[k0 14*3+mod(k0,14)];
            else
                Set3=[k0];
            end

            for l= 1:14
                [row col]=find((l~=[Set1,Set2,Set3])==0);
                if isempty(col)
                    SS=[abs(S(l,i0)/S(i0,i0)) abs(S(l,j0)/S(j0,j0)) abs(S(l,k0)/S(k0,k0))];
```

```
            [m n]=max(SS);
            if n==1
               Set1=[Set1 l 14*3+l];
            elseif n==2
               Set2=[Set2 l 14*3+l];
            elseif n==3
               Set3=[Set3 l 14*3+l];
            end
         end
      end
      for l= 15:42
         [row col]=find((l~=[Set1,Set2,Set3])==0);
         if isempty(col)
            SS=[abs(S(l,i0)/S(i0,i0)) abs(S(l,j0)/S(j0,j0)) abs(S(l,k0)/S(k0,k0))];
            [m n]=max(SS);
               if n==1
                  Set1=[Set1 l];
               elseif n==2
                  Set2=[Set2 l];
               elseif n==3
                  Set3=[Set3 l];
            end
         end
      end
      for l= 57:72
         [row col]=find((l~=[Set1,Set2,Set3])==0);
         if isempty(col)
            SS=[abs(S(l,i0)/S(i0,i0)) abs(S(l,j0)/S(j0,j0)) abs(S(l,k0)/S(k0,k0))];
               [m n]=max(SS);
               if n==1
                  Set1=[Set1 l];
               elseif n==2
                  Set2=[Set2 l];
               elseif n==3
                  Set3=[Set3 l];
            end
         end
      end

T=sqrt((1/72)*(sum((S(Set1,i0)/S(i0,i0)).^2)+sum((S(Set2,j0)/S(j0,j0)).^2)+sum((S(Set3,
k0)/S(k0,k0)).^2)));
      Num=[size(Set1'); size(Set2'); size(Set3')];
      Av=(1/3)*sum(Num(:,1));
      E=sqrt((1/3)*sum((Num(:,1)-Av).^2));
      J=(1/24)*E-T;
      if J<J0
```

```
            J0=J;
            best=[i0,j0,k0];
        end
    end
  end
end

i0=best(1);j0=best(2);k0=best(3);

 % Reconstructs the optimum partitioning
  if (i0<=42 && i0>=57)
            Set1=[i0 14*3+mod(i0,14)];
        else
            Set1=[i0];
        end
        if (j0<=42 && j0>=57)
            Set2=[j0 14*3+mod(j0,14)];
        else
            Set2=[j0];
        end
        if (k0<=42 && k0>=57)
            Set3=[k0 14*3+mod(k0,14)];
        else
            Set3=[k0];
        end

        for l= 1:14
            [row col]=find((l~=[Set1,Set2,Set3])==0);
            if isempty(col)
                SS=[abs(S(l,i0)/S(i0,i0)) abs(S(l,j0)/S(j0,j0)) abs(S(l,k0)/S(k0,k0))];
                [m n]=max(SS);
                if n==1
                    Set1=[Set1 l 14*3+l];
                elseif n==2
                    Set2=[Set2 l 14*3+l];
                elseif n==3
                    Set3=[Set3 l 14*3+l];
                end
            end
        end
        for l= 15:42
            [row col]=find((l~=[Set1,Set2,Set3])==0);
            if isempty(col)
                SS=[abs(S(l,i0)/S(i0,i0)) abs(S(l,j0)/S(j0,j0)) abs(S(l,k0)/S(k0,k0))];
                [m n]=max(SS);
                    if n==1
```

```
                Set1=[Set1 l];
            elseif n==2
                Set2=[Set2 l];
            elseif n==3
                Set3=[Set3 l];
            end
        end
    end
    for l= 57:72
        [row col]=find((l~=[Set1,Set2,Set3])==0);
        if isempty(col)
            SS=[abs(S(l,i0)/S(i0,i0)) abs(S(l,j0)/S(j0,j0)) abs(S(l,k0)/S(k0,k0))];
                [m n]=max(SS);
                if n==1
                    Set1=[Set1 l];
                elseif n==2
                    Set2=[Set2 l];
                elseif n==3
                    Set3=[Set3 l];
            end
        end
    end

 SET1=[];
[r1 c1]=size(Set1);
for i=1:c1
   [ms1 ns1]=min(Set1);
   SET1=[SET1 ms1];
   Set1=[Set1(1,1:ns1-1) Set1(1,ns1+1:end)];
end
SET2=[];
[r2 c2]=size(Set2);
for i=1:c2
   [ms2 ns2]=min(Set2);
   SET2=[SET2 ms2];
   Set2=[Set2(1,1:ns2-1) Set2(1,ns2+1:end)];
end
SET3=[];
[r3 c3]=size(Set3);
for i=1:c3
   [ms3 ns3]=min(Set3);
   SET3=[SET3 ms3];
   Set3=[Set3(1,1:ns3-1) Set3(1,ns3+1:end)];
end

% Creates sub-systems for controller design
```

```
A1=[];
for i=1:c1
   for j=1:c1
   A1(i,j)=A(SET1(i),SET1(j));
   end
end
A2=[];
for i=1:c2
   for j=1:c2
   A2(i,j)=A(SET2(i),SET2(j));
   end
end
A3=[];
for i=1:c3
   for j=1:c3
   A3(i,j)=A(SET3(i),SET3(j));
   end
end

[rp cp1 vp]=find(SET1>=57 & SET1<=70);
[ri ci1 vi]=find(SET1>=43 & SET1<=56);
[rcp ccp1]=size(cp1);
if isempty(cp1)
   C1=zeros(14,c1);
   Q1=eye(c1);
else
   SET1p=zeros(1,14); SET1p(1,SET1(1,cp1)-56)=p0(SET1(1,cp1)-56,1)';
   C11=diag(SET1p);I1=[]; for i=1:14 if sum(C11(:,i)~=zeros(14,1)); I1=[I1 i]; end; end;
C11=C11(:,I1);
   C1=[zeros(14,cp1(1)-1) C11 zeros(14,c1-cp1(end))];
   Q1=C1'*C1;
end
[rci1 cci1]=size(ci1);
if isempty(ci1)
   B1=zeros(c1,14);
else
   SET1i=zeros(1,14); SET1i(1,SET1(1,ci1)-42)=ones(1,cci1);
   B11=diag(SET1i);Ii1=[]; for i=1:14 if sum(B11(:,i)~=zeros(14,1)); Ii1=[Ii1 i]; end;
end; B11=B11(:,Ii1);
   B1=[zeros(ci1(1)-1,14);B11';zeros(c1-ci1(end),14)];
end

[rp cp2 vp]=find(SET2>=57 & SET2<=70);
[ri ci2 vi]=find(SET2>=43 & SET2<=56);
[rcp ccp2]=size(cp2);
if isempty(cp2)
```

```
   C2=zeros(14,c2);
   Q2=eye(c2);
else
   SET2p=zeros(1,14); SET2p(1,SET2(1,cp2)-56)=p0(SET2(1,cp2)-56,1)';
   C22=diag(SET2p);I2=[]; for i=1:14 if sum(C22(:,i)~=zeros(14,1)); I2=[I2 i]; end; end;
C22=C22(:,I2);
   C2=[zeros(14,cp2(1)-1) C22 zeros(14,c2-cp2(end))];
   Q2=C2'*C2;
end
[rci2 cci2]=size(ci2);
if isempty(ci2)
   B2=zeros(c2,14);
else
   SET2i=zeros(1,14); SET2i(1,SET2(1,ci2)-42)=ones(1,cci2);
   B22=diag(SET2i);Ii2=[]; for i=1:14 if sum(B22(:,i)~=zeros(14,1)); Ii2=[Ii2 i]; end;
end; B22=B22(:,Ii2);
   B2=[zeros(ci2(1)-1,14);B22';zeros(c2-ci2(end),14)];
end

[rp cp3 vp]=find(SET3>=57 & SET3<=70);
[ri ci3 vi]=find(SET3>=43 & SET3<=56);
[rcp ccp3]=size(cp3);
if isempty(cp3)
   C3=zeros(14,c3);
   Q3=eye(c3);
else
   SET3p=zeros(1,14); SET3p(1,SET3(1,cp3)-56)=p0(SET3(1,cp3)-56,1)';
   C33=diag(SET3p);I3=[]; for i=1:14 if sum(C33(:,i)~=zeros(14,1)); I3=[I3 i]; end; end;
C33=C33(:,I3);
   C3=[zeros(14,cp3(1)-1) C33 zeros(14,c3-cp3(end))];
   Q3=C3'*C3;
end
[rci3 cci3]=size(ci3);
if isempty(ci3)
   B3=zeros(c3,14);
else
   SET3i=zeros(1,14); SET3i(1,SET3(1,ci3)-42)=ones(1,cci3);
   B33=diag(SET3i);Ii3=[]; for i=1:14 if sum(B33(:,i)~=zeros(14,1)); Ii3=[Ii3 i]; end;
end; B33=B33(:,Ii3);
   B3=[zeros(ci3(1)-1,14);B33';zeros(c3-ci3(end),14)];
end

if B1==0
   K1=zeros(14,14);
else
   [P1,L1,K1] = care(A1,B1,Q1);
```

```
end
if B2==0
   K2=zeros(14,14);
else
   [P2,L2,K2] = care(A2,B2,Q2);
end
if B3==0
   K3=zeros(14,14);
else
   [P3,L3,K3] = care(A3,B3,Q3);
end

[nr1, nc1]=size(K1);
[nr2, nc2]=size(K2);
[nr3, nc3]=size(K3);

K_add=zeros(14,72);K_add(:,SET1)=K1;K_add(:,SET2)=K2;K_add(:,SET3)=K3;

nA1=size(A1); nA2=size(A2); nA3=size(A3);
[LP1,LL1,LK1] = care(A1',C1',eye(nA1(1)));
[LP2,LL2,LK2] = care(A2',C2',eye(nA2(1)));
[LP3,LL3,LK3] = care(A3',C3',eye(nA3(1)));

[P,L,K] = care(A,B,C'*C);
[LP,LL,LK] = care(A',C',eye(72));

K1_c=zeros(nr1, nc1);
K1_c(find(SET1i==1),1:nc1)=K(find(SET1i==1),SET1);
K2_c=zeros(nr2, nc2);
K2_c(find(SET2i==1),1:nc2)=K(find(SET2i==1),SET2);
K3_c=zeros(nr3, nc3);
K3_c(find(SET3i==1),1:nc3)=K(find(SET3i==1),SET3);
```

References

[1] R. H. Prinsloo, D. I. Tomasevic, "The Analytical Nodal Method in Cylindrical Geometry," Nuclear Engineering and Design, Vol. 238, No. 11, pp.2898-2907, 2008.

[2] A. P. Tiwari, B. Bandyopadhyay, G. Govindarajan, "Spatial Control of a Large Pressurized Heavy Water Reactor," IEEE Transactions on Nuclear Science, Vol. 43, No. 4, pp.2440-2453, 1996.

[3] A. P. Tiwari, "Modeling and Control of a Large Pressurized Heavy Water Reactor," Ph.D. Dissertation, Indian Institute of Technology, Bombay, India, 1999.

[4] D. B. Talange, B. Bandyopadhyay, A. P. Tiwari, "Spatial Control of a Large PHWR by Decentralized Periodic Output Feedback and Model Reduction Techniques," IEEE Transactions on Nuclear Science, Vol. 53, No. 4, pp.2308-2317, 2006.

[5] S. S. Bajaj, A. R. Gore, "The Indian PHWR," Nuclear Engineering and Design, Vol. 236, Issues 7-8, pp.701-722, 2006.

[6] B. Rouben, "Introduction to Reactor Physics," Atomic Energy of Canada Limited, September 2002.

[7] J. Zhang, R. A. Olmstead, "Reactor Control Systems of Qinshan Phase III CANDU Nuclear Plant," CJNPE, 2005.

[8] A. P. Tiwari, B. Bandyopadhyay, "Control of Xenon Induced Spatial Oscillations in a Large PHWR," *TENCOM '98. 1998 IEEE Region 10 International Conference on Global Connectivity in Energy, Computer, Communication and Control*, New Delhi, India, December 17-19, 1998.

[9] H. Javidnia , J. Jiang, M. Borairi, "Modeling and Simulation of a CANDU Reactor for Control System Design and Analysis," Nuclear Technology, Vol. 165, No. 2, pp.174-189 ,2009.

[10] D. B. Talange, B. Bandyopadhyay, A. P. Tiwari, "Spatial Control of a Large PHWR via Reduced Model," Nuclear Technology, Vol. 138, pp.217-237, 2002.

[11] J. J. Duderstadt, L. J. Hamilton, *Nuclear Reactor Analysis*, John Wiley and Sons, Inc., New York, 1976.

[12] C. Lee, "The Network Architecture and Site Test of DCIS in Lungmen Nuclear Power Station," *ANS NPIC&HMIT 2006 Topical Meeting Proceedings*, Albuquerque, NM, November 12-16, American Nuclear Society, 2006.

[13] D. Chaniotis, M. A. Pai, “Model Reduction in Power Systems using Krylov Subspace Methods,” IEEE Transactions on Power Systems, Vol. 20, No.2, pp.888-894, 2005.

[14] E. J. Davison, “A Method for Simplifying Linear Dynamic Systems,” IEEE Transactions on Automatic Control, Vol. 11, No. 1, pp.93-101, 1966.

[15] J. Lai, J. Hung, “Practical Model Reduction Methods,” IEEE Transactions on Industrial Electronics, Vol. IE-24, No. 1, pp.70-77, 1987.

[16] M. L. J. Hautus, M. Heymann, “Linear Feedback Decoupling-Transfer Function Analysis,” IEEE Transactions on Automatic Control, Vol. AC-28, No. 8, pp.823-832, 1983.

[17] E. Fabian, W. M. Wonham, “Decoupling and Data Sensitivity,” IEEE Transactions on Automatic Control, Vol. AC-20, No. 3, pp.338-344, 1975.

[18] B. G. Mertzios, M. A. Christodoulou, “Decoupling and Data Sensitivity in Singular Systems,” IEE Proceedings, Vol. 135, Pt. D, No. 2, pp.106-110, 1988.

[19] W. Wang, Y. Zhang, Y. Li, X. Zhang, “The Global Fuzzy C-Means Clustering Algorithm,” *Proceedings of the 6th World Congress on Intelligent Control*, Dalian, China, June 21-23, 2006.

[20] R. R. Yager, D. P. Filev, “Essentials of Fuzzy Modeling and Control,” John Wiley and Sons, Inc., New York, 1994.

[21] I. T. Jollife, “Principal Component Analysis: Second Edition,” Springer-Verlag New York Inc., New York, 2002.

[22] R. Miklosovic, Z. Gao, "A Dynamic Decoupling Method for Controlling High Performance Turbofan Engines," *Proceedings of 2005 IFAC World Congress*, Prague, July, 2005.

[23] D. B. Talange, “Modeling and Spatial Control of a Large Nuclear Reactor with Reactivity Feedback Effects,” Ph.D. Dissertation, Indian Institute of Technology, Bombay, India, 2004.

[24] Z. M. Bi, W. J. Zhang, “Concurrent Optimal Design of Modular Robotic Configuration,” Journal of Robotic Systems, Vol. 18, Issue 2, pp.77-87, 2001.

[25] A. H. Chaudhry, B. A. Francis, G. J. Rogers, “Retaining States of the Original System in Reduced Order Model,” *IEEE Power Engineering Society 1999 Winter Meeting Proceedings*, New York, USA, January 31-February 4, 1999.

[26] N. Khan, "Distributed Control System Implementation in Nuclear Power Plants Worldwide: A Literature Survey," *Proceedings of the 32nd Student Conference of the Canadian Nuclear Society/Canadian Nuclear Association*, Toronto, Canada, June 1-4, 2008.

[27] N. Khan, L. Lu, "Design of a Decoupling Algorithm for the Reactor Nodal Core Model of a Large PHWR," *Proceedings of the 30th Annual Conference of the Canadian Nuclear Society*, Calgary, Canada, May 31-June 3, 2009.